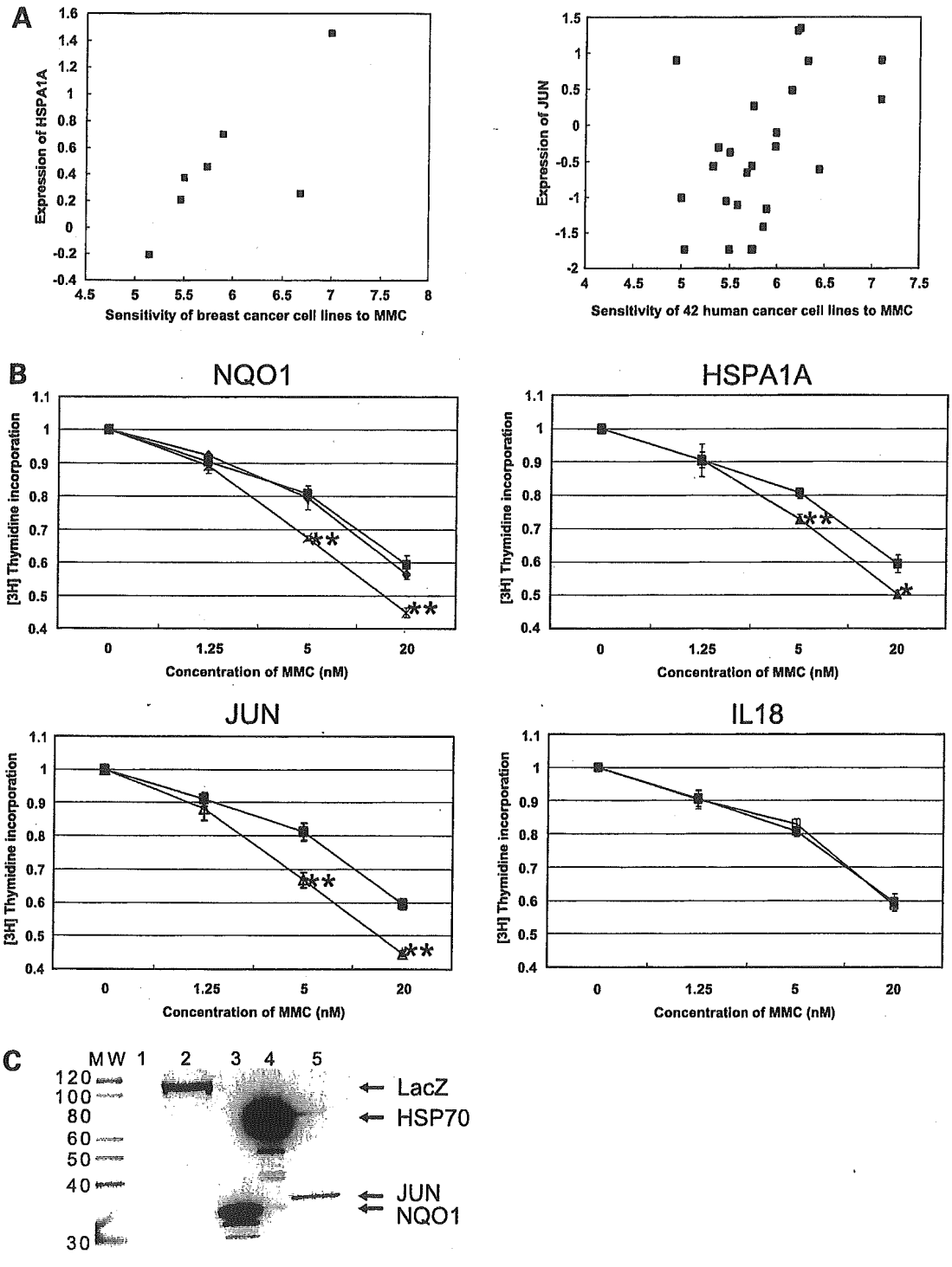

Figure 3. Relationships between MMC sensitivity and expression of HSPA1A in breast cancer cell lines (**A**, *left*) or JUN in 42 cell lines (**A**, *right*). Each symbol indicates one cell line. *X axis,* MMC sensitivity; *Y axis,* expression of HSPA1A or JUN. Pearson correlation coefficients between MMC sensitivity and expression of HSPA1A and JUN were 0.75 ($P = 0.05$) and 0.473 ($P = 0.015$), respectively. **B**, growth inhibition curves by MMC in mock (■), LacZ (♦), NQO1 (×), HSPA1A (▲), JUN (△), or IL-18 (□) transfected HT1080 cells. This growth inhibition by MMC was enhanced in HT1080 cells transfected with NQO1, HSPA1A, and JUN. *, $P < 0.002$; **, $P < 0.0001$, *t* test against mock-transfected cells. **C**, expressions of genes were certified by immunoblotting with anti-*myc* antibody: *myc*-tagged LacZ (*lane 2*), NQO1 (*lane 3*), 70-kDa heat shock protein (*HSP70; lane 4*), and JUN (*lane 5*).

ref. 32) and showed that drugs with similar modes of actions were classified into the same cluster by hierarchical clustering (19). In this study, we constructed a new panel of 45 human cancer cell lines (JFCR-45), comprising cancer cell lines derived from tumors from three different organ types: breast, liver, and stomach. In particular, the inclusion of cell lines derived from gastric and hepatic cancers is a major point of novelty. JFCR-45 can be used for analyzing both organ-specific differences in chemosensitivity and intraorgan heterogeneity of chemosensitivity. We examined 53 anticancer drugs for their activity against JFCR-45 and observed differential activity across the whole panel as well as within a single organ type (e.g., breast, liver, or stomach). Furthermore, as shown in Fig. 1, using JFCR-45, drugs with a similar mode of action (such as a tubulin binder or topo I inhibitor) were classified into the same cluster, which were the same as the clusters established for NCI-60 (35) and JFCR-39 (19). These results suggest that the cell line panel-based assessment system is generally effective for classifying anticancer drugs with the same modes of action into the same set of clusters.

In this study, we investigated the gene expression profiles of 42 cell lines of JFCR-45 using cDNA array consisting of 3,537 genes. Hierarchical clustering analysis of these gene expression profiles classified organ-specific cell lines mostly into the same cluster, suggesting that these cell lines maintained the genetic characteristics of the parent organ as far as the gene expression profiles were concerned.

We did a Pearson correlation analysis of the gene expression database and the drug sensitivity database. Consequently, many genes whose expressions were correlated with respect to the sensitivity of each drug were identified. For example, DNA alkylating agents and nucleic acid–related genes, including *SF1* encoding ZFM1, *c-JUN* oncogene, and *SFRS9* were extracted as the genes sensitive to MMC. The genes that were sensitive to paclitaxel included tubulin binder and cytoskeleton-related genes, such as *VIL2* encoding ezrin and *ACTB* encoding β-actin.

These results suggest that the extracted genes are the predictive markers of drug efficacy. We further applied Pearson correlation analysis to each type (i.e., breast, liver, or stomach cancer) of cell lines. There were two advantages in this type of analysis: one is that we could compare the cell lines having the same organ background and another is that organ-specific genes, which worked as the sensitive or resistant factors, could be extracted. For example, for MMC, several genes (such as *INHBB*, *NK4*, and *HSPA1A*) were newly extracted as candidate genes sensitive to MMC from the breast cancer cell lines. Surprisingly, compared with the breast and liver cancer cells, many new candidate genes were extracted from the stomach cancer cell lines. These extracted genes were considered as the candidates for organ-specific predictive markers of drug efficacy.

We hypothesized that some of the candidate sensitivity genes described above might causally affect the chemosensitivity of cancer cell lines. To validate this possibility, we selected 19 genes, including *HSPA1A*, *JUN*, and *IL-18*, and examined whether the expression of these candidate genes would affect the cellular sensitivity to anticancer drugs. Overexpression of 2 of the 19 genes, *HSPA1A* encoding 70-kDa heat shock protein and *JUN* encoding c-JUN, indeed enhanced cellular sensitivity to MMC in HT1080 cells (Fig. 3), suggesting that they function to mediate MMC sensitivity. This was an unexpected finding, because a direct relationship between these two genes and MMC sensitivity has not been reported previously, although a relationship between heat shock protein and cancer has been suggested previously (36, 37). How these two genes potentiate MMC sensitivity remains to be clarified. In this validation, we used the HT1080 cell line instead of those in JFCR-45 because of its high transfection efficiency. As the alteration of chemosensitivity following the overexpression of any particular gene may depend highly on the genotypic/phenotypic background of the transfected HT1080 cells, further validation using cell lines within JFCR-45 will be required. In addition to the overexpression experiments, validation by silencing chemosensitivity-related genes using small interfering RNA will be required.

Pioneering attempts to discover new leads and targets and to investigate new aspects of the molecular pharmacology of anticancer drugs by mining the NCI-60 database have been done (31, 33-35). Recently, Szakacs et al. (38) have identified interesting compounds whose activity is potentiated by the MDR1 multidrug transporter. Our previous studies using JFCR-39 (19, 20, 31) and the present study using JFCR-45 also indicate that a comprehensive analysis of chemosensitivity and gene expression data followed by experimental validation leads to the identification of genes that determine drug sensitivity.

In conclusion, we established a sensitivity database for JFCR-45, which focused on organ origin, to 53 anticancer drugs. Using JFCR-45, anticancer drugs were classified according to their modes of action. Moreover, we established a database of the gene expression profiles in 42 cell lines of JFCR-45. Using these two databases, we have identified several genes that may predict chemosensitivity of cancer. Among these candidate genes, we identified two genes, *HSPA1A* and *JUN*, which determined sensitivity to MMC. Thus, this approach is useful not only to discover predictive markers for the efficacy of anticancer drugs but also to discover genes that determine chemosensitivity.

Acknowledgments

We thank Yumiko Mukai, Yumiko Nishimura, Mariko Seki, and Fujiko Ohashi for the determination of chemosensitivity and Dr. Munetika Enjoji (Department of Internal Medicine, National Kyushu Cancer Center, Fukuoka, Japan) for providing the RBE and SSP-25 cell lines.

References

1. Chen CJ, Clark D, Ueda K, et al. Genomic organization of the human multidrug resistance (MDR1) gene and origin of P-glycoproteins. J Biol Chem 1990;265:506–14.

2. Taniguchi K, Wada M, Kohno K, et al. A human canalicular multispecific organic anion transporter (cMOAT) gene is overexpressed in cisplatin-resistant human cancer cell lines with decreased drug accumulation. Cancer Res 1996;56:4124–9.

3. Kool M, de Haas M, Scheffer GL, et al. Analysis of expression of cMOAT (MRP2), MRP3, MRP4, and MRP5, homologues of the multidrug

resistance-associated protein gene (MRP1), in human cancer cell lines. Cancer Res 1997;57:3537–47.

4. Patterson LH, Murray GI. Tumour cytochrome *P*450 and drug activation. Curr Pharm Des 2002;8:1335–47.

5. Batist G, Tulpule A, Sinha BK, et al. Overexpression of a novel anionic glutathione transferase in multidrug-resistant human breast cancer cells. J Biol Chem 1986;261:15544–9.

6. Meisel P. Arylamine *N*-acetyltransferases and drug response. Pharmacogenomics 2002;3:349–66.

7. Nair MG, Baugh CM. Synthesis and biological evaluation of poly-γ-glutamyl derivatives of methotrexate. Biochemistry 1973;12:3923–7.

8. Schimke RT. Methotrexate resistance and gene amplification. Mechanisms and implications. Cancer 1986;57:1912–7.

9. Pinedo HM, Peters GF. Fluorouracil: biochemistry and pharmacology. J Clin Oncol 1988;6:1653–64.

10. Eastman A. Mechanisms of resistance to cisplatin. Cancer Treat Res 1991;57:233–49.

11. Cohen SS. The mechanisms of lethal action of arabinosyl cytosine (araC) and arabinosyl adenine (araA). Cancer 1977;40:509–18.

12. Gustafson DL, Pritsos CA. Enhancement of xanthine dehydrogenase mediated mitomycin C metabolism by dicumarol. Cancer Res 1992;52:6936–9.

13. Kang HC, Kim IJ, Park JH, et al. Identification of genes with differential expression in acquired drug-resistant gastric cancer cells using high-density oligonucleotide microarrays. Clin Cancer Res 2004;10:272–84.

14. Sato T, Odagiri H, Ikenaga SK, et al. Chemosensitivity of human pancreatic carcinoma cells is enhanced by IκBα super-repressor. Cancer Sci 2003;94:467–72.

15. Zembutsu H, Ohnishi Y, Tsunoda T, et al. Genome-wide cDNA microarray screening to correlate gene expression profiles with sensitivity of 85 human cancer xenografts to anticancer drugs. Cancer Res 2002;62:518–27.

16. Okutsu J, Tsunoda T, Kaneta Y, et al. Prediction of chemosensitivity for patients with acute myeloid leukemia, according to expression levels of 28 genes selected by genome-wide complementary DNA microarray analysis. Mol Cancer Ther 2002;1:1035–42.

17. Tanaka T, Tanimoto K, Otani K, et al. Concise prediction models of anticancer efficacy of 8 drugs using expression data from 12 selected genes. Int J Cancer 2004;111:617–26.

18. Scherf U, Ross DT, Waltham M, et al. A gene expression database for the molecular pharmacology of cancer. Nat Genet 2000;24:236–44.

19. Dan S, Tsunoda T, Kitahara O, et al. An integrated database of chemosensitivity to 55 anticancer drugs and gene expression profiles of 39 human cancer cell lines. Cancer Res 2002;62:1139–47.

20. Dan S, Shirakawa M, Mukai Y, et al. Identification of candidate predictive markers of anticancer drug sensitivity using a panel of human cancer cell lines. Cancer Sci 2003;94:1074–82.

21. Kurebayashi J, Kurosumi M, Sonoo H. A new human breast cancer cell line, KPL-3C, secretes parathyroid hormone-related protein and produces tumours associated with microcalcifications in nude mice. Br J Cancer 1996;74:200–7.

22. Shiu RP. Processing of prolactin by human breast cancer cells in long term tissue culture. J Biol Chem 1980;255:4278–81.

23. Engel LW, Young NA, Tralka TS, et al. Establishment and characterization of three new continuous cell lines derived from human breast carcinomas. Cancer Res 1978;38:3352–64.

24. Dor I, Namba M, Sato J. Establishment and some biological characteristics of human hepatoma cell lines. Gann 1975;66:385–92.

25. Tanaka M, Kawamura K, Fang M, et al. Production of fibronectin by HUH6 C15 cell line established from a human hepatoblastoma. Biochem Biophys Res Commun 1983;110:837–41.

26. Fukutomi M, Enjoji M, Iguchi H, et al. Telomerase activity is repressed during differentiation along the hepatocytic and biliary epithelial lineages: verification on immortal cell lines from the same origin. Cell Biochem Funct 2001;19:65–8.

27. Sorimachi K, Hayashi T, Takaoka T, et al. Requirement of serum pretreatment for induction of alkaline phosphatase activity with prednisolone, butyrate, dibutyryl cyclic adenosine monophosphate and NaCl in human liver cells continuously cultured in serum-free medium. Cell Struct Funct 1988;13:1–11.

28. Fujise K, Nagamori S, Hasumura S, et al. Integration of hepatitis B virus DNA into cells of six established human hepatocellular carcinoma cell lines. Hepatogastroenterology 1990;37:457–60.

29. Imanishi K, Yamaguchi K, Suzuki M, et al. Production of transforming growth factor-α in human tumour cell lines. Br J Cancer 1989;59:761–5.

30. Yamori T, Matsunaga A, Sato S, et al. Potent antitumor activity of MS-247, a novel DNA minor groove binder, evaluated by an *in vitro* and *in vivo* human cancer cell line panel. Cancer Res 1999;59:4042–9.

31. Monks A, Scudiero D, Skehan P, et al. Feasibility of a high-flux anticancer drug screen using a diverse panel of cultured human tumor cell lines. J Natl Cancer Inst 1991;83:757–66.

32. Yamori T. Panel of human cancer cell lines provides valuable database for drug discovery and bioinformatics. Cancer Chemother Pharmacol 2003;52 Suppl 1:S74–9.

33. Paull KD, Shoemaker RH, Hodes L, et al. Display and analysis of patterns of differential activity of drugs against human tumor cell lines: development of mean graph and COMPARE algorithm. J Natl Cancer Inst 1989;81:1088–92.

34. Weinstein JN, Kohn KW, Grever MR, et al. Neural computing in cancer drug development: predicting mechanism of action. Science 1992;258:447–51.

35. Weinstein JN, Myers TG, O'Connor PM, et al. An information-intensive approach to the molecular pharmacology of cancer. Science 1997;275:343–9.

36. Laroia G, Cuesta R, Brewer G, et al. Control of mRNA decay by heat shock-ubiquitin-proteasome pathway. Science 1999;284:499–502.

37. Jolly C, Morimoto RI. Role of the heat shock response and molecular chaperones in oncogenesis and cell death. J Natl Cancer Inst 2000;92:1564–72.

38. Szakacs G, Annereau JP, Lababidi S, et al. Predicting drug sensitivity and resistance: profiling ABC transporter genes in cancer cells. Cancer Cell 2004;6:129–37.

Oncogene (2004) 23, 6914–6923

www.nature.com/onc

Negative regulation of transforming growth factor-β (TGF-β) signaling by WW domain-containing protein 1 (WWP1)

Akiyoshi Komuro[1,2], Takeshi Imamura[2,3], Masao Saitoh[1], Yoko Yoshida[4], Takao Yamori[4], Kohei Miyazono[1,3] and Keiji Miyazawa*[,1]

[1]*Department of Molecular Pathology, Graduate School of Medicine, University of Tokyo, 7-3-1 Hongo, Bunkyo-ku, Tokyo 113-0033, Japan;* [2]*Department of Biological Sciences, Graduate School of Bioscience and Biotechnology, Tokyo Institute of Technology, Nagatsuta, Yokohama 226-8501, Japan;* [3]*Department of Biochemistry;* [4]*Cancer Chemotherapy Center, The Cancer Institute of the Japanese Foundation for Cancer Research (JFCR), 1-37-1 Kami-ikebukuro, Toshima-ku, Tokyo 170-8455, Japan*

Smad7 negatively regulates transforming growth factor (TGF)-β superfamily signaling by binding to activated type I receptors, thereby preventing the phosphorylation of receptor-regulated Smads (R-Smads), as well as by recruiting HECT-type E3 ubiquitin ligases to degrade type I receptors through a ubiquitin-dependent mechanism. To elucidate the regulatory mechanisms of TGF-β signaling, we searched for novel members of proteins that interact with Smad7 using a yeast two-hybrid system. One of the proteins identified was the WW domain-containing protein 1 (WWP1) that is structurally related to Smad ubiquitin regulatory factors (Smurfs), E3 ubiquitin ligases for Smads and TGF-β superfamily receptors. Using a TGF-β-responsive reporter in mammalian cells, we found that WWP1 inhibited transcriptional activities induced by TGF-β. Similar to Smurfs, WWP1 associated with Smad7 and induced its nuclear export, and enhanced binding of Smad7 to TGF-β type I receptor to cause ubiquitination and degradation of the receptor. Consistent with these results, WWP1 inhibited phosphorylation of Smad2 induced by TGF-β. WWP1 thus negatively regulates TGF-β signaling in cooperation with Smad7. However, unlike Smurfs, WWP1 failed to ubiquitinate R-Smads and SnoN. Importantly, WWP1 and Smurfs were expressed in distinct patterns in human tissues and carcinoma cell lines, suggesting unique pathophysiological roles of WWP1 and Smurfs.
Oncogene (2004) **23,** 6914–6923. doi:10.1038/sj.onc.1207885
Published online 28 June 2004

Keywords: WWP1; Smurfs; ubiquitin-proteasome pathway; Smad7; TGF-β

Introduction

Members of the transforming growth factor-β (TGF-β) superfamily, including TGF-β, activin, nodal, and bone morphogenetic proteins (BMPs) are multifunctional proteins that regulate cellular growth, differentiation, apoptosis, and morphogenesis (Roberts and Sporn, 1990). Since TGF-β acts as a potent growth inhibitor, loss of TGF-β signaling has been thought to play a role in tumorigenesis (Massagué *et al.*, 2000). TGF-β and related proteins bind to two types of serine/threonine kinase receptors, type I and type II, and transduce signals principally through Smad proteins (Heldin *et al.*, 1997; Derynck *et al.*, 1998; Attisano and Wrana, 2000). In mammals, eight Smads have been identified and classified into three groups; receptor-regulated Smads (R-Smads), common-partner Smads (Co-Smads), and inhibitory Smads (I-Smads). Among these, R-Smads and Co-Smads positively regulate TGF-β superfamily signals. Upon phosphorylation by type I receptors, R-Smads form heteromeric complexes with Co-Smad (Smad4), and translocate into the nucleus. Nuclear Smad complexes bind to transcription factors as well as coactivators/corepressors, and regulate transcription of target genes (Miyazawa *et al.*, 2002). Among the R-Smads, Smad2 and Smad3 act in the TGF-β, activin and Nodal pathways, whereas Smad1, Smad5, and Smad8 act in the BMP pathway. I-Smads, including Smad6 and Smad7, are induced by TGF-β superfamily ligands, bind to type I receptors, and prevent phosphorylation of R-Smads, resulting in the inhibition of TGF-β superfamily signaling (Imamura, *et al.*, 1997; Hanyu *et al.*, 2001).

Recently, several reports have demonstrated that Smad ubiquitin regulatory factors (Smurfs) negatively regulate TGF-β superfamily signaling. Smurf1 was originally identified as a homologue of the E6AP C terminus (HECT)-type E3 ubiquitin ligases that induces ubiquitination and degradation of Smad1 (Zhu *et al.*, 1999). Smurf2, a Smurf1-related E3 ubiquitin ligase, interacts with both Smad1 and Smad2, and induces their ubiquitin-mediated degradation (Lin *et al.*, 2000; Zhang *et al.*, 2001). In contrast, Bonni *et al.* (2001) demonstrated that Smurf2 does not effectively induce degradation of Smad2, and that Smurf2 binds to transcriptional corepressor SnoN via Smad2, leading to ubiquitin-mediated degradation of SnoN. In addition, Smurfs 1 and 2 interact with Smad7 in the nucleus and induce translocation of Smad7 to the cytoplasm in a CRM-1-dependent fashion (Kavsak *et al.*, 2000; Ebisawa *et al.*, 2001; Tajima *et al.*, 2003). The Smurf1–Smad7 complex

*Correspondence: K Miyazawa; E-mail: keiji-miyazawa@umin.ac.jp
Received 10 January 2004; revised 5 May 2004; accepted 11 May 2004; published online 28 June 2004

is then targeted to the cell membrane through the C2 domain in Smurf1, and associates with TGF-β type I receptor (TβR-I) (Suzuki *et al.*, 2002). After binding to TβR-I, Smurfs 1 and 2 induce ubiquitin-mediated degradation of TβR-I.

WW domain-containing protein 1 (WWP1) was first identified as a novel protein with WW domains (Pirozzi *et al.*, 1997). The WW domain is a protein module consisting of 35–40 amino acids that has the ability to bind to the PY motif, a proline-rich sequence followed by a tyrosine residue. WWP1 shares a characteristic domain organization with Nedd4 and Smurfs, which consist of a C2 domain, 2–4 WW domains, and a HECT domain (Flasza *et al.*, 2002). Although WWP1 has been regarded as an E3 ubiquitin ligase, its substrates are yet to be determined. However, it has been reported that WWP1 regulates the function of Lung Krüppel-like factor (Conkright *et al.*, 2001) and that it is essential for embryonic development in *Caenorhabditis. elegans* (Huang *et al.*, 2000).

In the present study, we employed a yeast two-hybrid system to identify proteins that interact with Smad7, and found that one of the identified clones encoded WWP1. We have shown that WWP1 interacts with Smad7 and negatively regulates TGF-β signaling in cooperation with Smad7.

Results

*WWP1 inhibits transcriptional activity induced by TGF-*β

To identify proteins that play a regulatory role in TGF-β signaling, we performed a yeast two-hybrid screening of a human lung cDNA library using full-length Smad7 as bait. In total, we isolated 3000 positive clones from 3.0×10^6 transformants. Among the positive clones, we have identified one clone that encodes WWP1 lacking the N-terminal 294 amino acids (WWP1(del)) (Figure 1a). WWP1 is a member of the HECT-type E3 ubiquitin ligase family and shares structural similarities with Smurfs that contain a C2 domain at the N-terminus, WW domains in the middle region, and a HECT domain at the C-terminus. WWP1 has four WW domains, whereas Smurf1 and Smurf2 have two and three WW domains, respectively.

To examine the function of WWP1 in TGF-β signaling, we first cloned a full-length WWP1 cDNA and performed a luciferase reporter assay using a TGF-β-responsive reporter $(CAGA)_9$-MLP-Luc in transfected R mutant Mv1Lu (R4-2) cells (Figure 1b). WWP1 inhibited transcriptional activity induced by TβR-I(TD) in a dose-dependent manner although the inhibitory activity of WWP1 was weaker than that of Smurf1. Similar results were obtained in HepG2 cells (data not shown).

WWP1 interacts with Smad7 and induces translocation of Smad7 from the nucleus to the cytoplasm

WWP1 has four WW domains that may interact with PY motif, a proline-rich sequence followed by a tyrosine

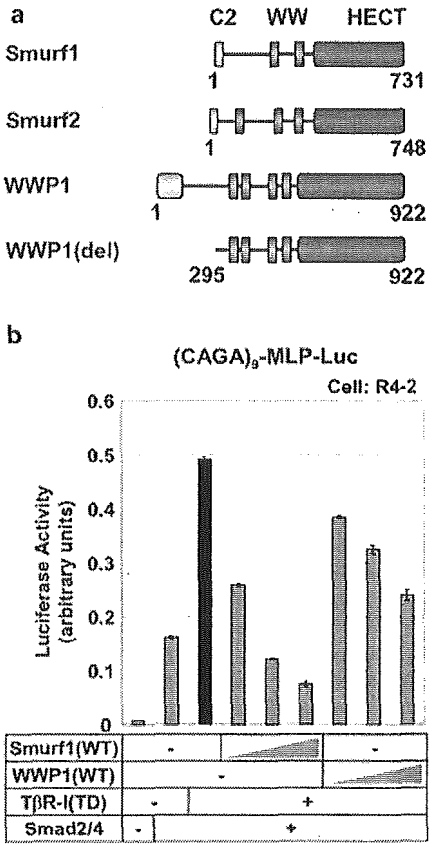

Figure 1 WWP1 as a negative regulator of TGF-β signaling. (**a**) Schematic representation of Smurf1, Smurf2, WWP1, and WWP1(del) that lacks the N-terminal 294 amino acids of WWP1. (**b**) WWP1 inhibits transcriptional activity induced by TβR-I(TD) in a dose-dependent manner. R mutant Mv1Lu (R4-2) cells were cotransfected with a $(CAGA)_9$-MLP-Luc construct and the plasmids indicated. Smurf1(WT) cDNA and WWP1(WT) cDNA were transfected at the doses of 0.2, 0.5, and 0.8 μg

residue. Smad proteins, with the exception of Smads 4 and 8, have a PY motif in their linker region. It was thus anticipated that WWP1 interacts with Smad proteins other than Smad7. We then examined the interaction of WWP1 with each of the Smad proteins in transfected COS7 cells, and compared the Smad-binding property of WWP1 with that of Smurf1 and 2 (Figure 2a). For this assay, a WWP1 mutant in which Cys-890 was replaced by alanine to abolish E3 ubiquitin ligase activity (WWP1(CA)) was used, in order to exclude the possibility that WWP1-induced ubiquitination/degradation of Smad proteins may affect the apparent binding profile of WWP1 to Smad proteins (Ebisawa *et al.*, 2001). Similar to Smurfs, WWP1(CA) effectively interacted with Smad6 and Smad7 but not with Smad4 and Smad8, both of which lack a PY motif. WWP1 and Smurfs have, however, distinct R-Smad-binding properties. WWP1(CA) associated with Smads 2 and 3 as efficiently as with Smad6 and 7, but only weakly with Smads 1 and 5, whereas both Smurfs(CA) strongly interacted with Smad1 and 5 in the presence of

constitutively active BMP-type IB receptor (BMPR-IB(QD)/ALK6(QD)).

We next examined the effect of WWP1 on the subcellular localization of Smad7 using immunohistochemical staining. WWP1(CA) was used because E3 ligase activity is not required for Smurf1-induced cytoplasmic translocation of Smad7 (Ebisawa *et al.*, 2001). When transfected alone into HeLa cells, Smurf1(-CA) as well as WWP1(CA) were mainly detected in the cytoplasm, and also gave weak staining in the nucleus (Figure 2b, lower two panels), whereas Smad7 mainly localized in the nucleus of HeLa cells (Figure 2b, top panels). In the presence of Smurf1(CA) or WWP1(CA), however, Smad7 was localized in the cytoplasm (Figure 2c). Similar results were obtained in HepG2 cells, R mutant Mv1Lu cells, and 293T cells (data not shown). These results indicate that WWP1 induces translocation of Smad7 from the nucleus to the cytoplasm.

WWP1 binds to TβR-I via Smad7and induces ubiquitin-mediated degradation of TβR-I

Previous studies have shown that Smurf1 and 2 interact with TβR-I via Smad7 and induce ubiquitin-mediated degradation of the receptor (Kavsak *et al.*, 2000; Ebisawa *et al.*, 2001). To examine whether WWP1 also binds to TβR-I, we performed an affinity crosslinking assay in transfected COS7 cells. In the presence of Smad7, [^{125}I]TGF-β-crosslinked receptor complexes were co-precipitated with WWP1(CA) (Figure 3a). The efficiency of co-precipitation was lower than that with Smurf1(CA) but similar to that with Smurf2(CA). Moreover, when Smad7 was immunoprecipitated, WWP1(CA) caused efficient co-precipitation of the TGF-β receptor complex (Figure 3b). We thus concluded that WWP1 binds to TβR-I via Smad7.

Next, we tested ubiquitination of TβR-I by the Smad7-WWP1 complex (Figure 4a). Ubiquitination of

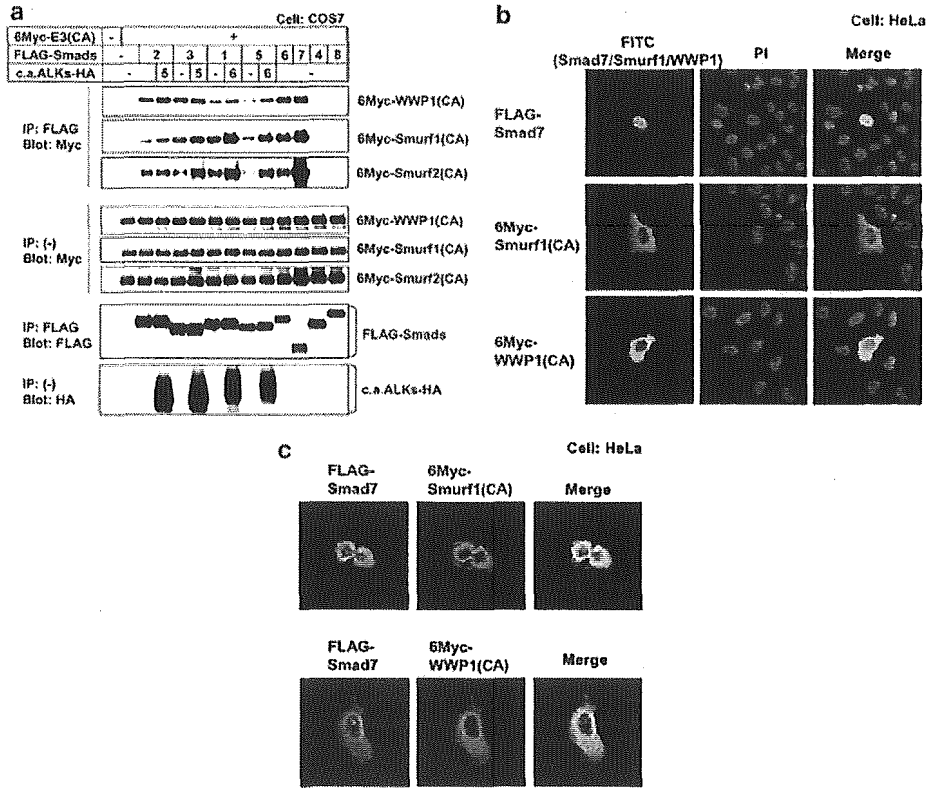

Figure 2 WWP1 interacts with Smad7 and recruits Smad7 from the nucleus to the cytoplasm. (a) Interaction of WWP1(CA), Smurf1(CA), or Smurf2(CA) with various Smad proteins. COS7 cells were transfected with the indicated plasmids. Smad proteins were immunoprecipitated with anti-FLAG antibody, followed by immunoblotting to visualize the coprecipitated proteins using anti-Myc antibody. The top three panels show the interaction, and the lower five panels the expression, of each protein as indicated. Since expression levels of FLAG-Smads and c.a.ALKs-HA were similar in the three experiments using WWP1(CA), Smurf1(CA), and Smurf2(CA), data using WWP1(CA) were shown in this figure. 6Myc-E3(CA) indicates either of WWP1(CA), Smurf1(CA), or Smurf2(CA). c.a.ALKs denotes constitutively active activin receptor-like kinases (ALKs). (**b**) Subcellular localization of Smad7, Smurf1(CA), and WWP1(CA). HeLa cells were transiently transfected with FLAG-tagged Smad7, 6Myc-tagged Smurf1(CA), or 6Myc-tagged WWP1(CA). Cells were fixed and stained as described in 'Materials and methods'. FLAG-tagged and 6Myc-tagged proteins are shown in green and nuclear staining by propidium iodide (PI) is shown in red. (**c**) WWP1(CA) recruits Smad7 from the nucleus to the cytoplasm. HeLa cells were transfected with FLAG-Smad7 together with 6Myc-Smurf1(CA) (top panels) or 6Myc-WWP1(CA) (lower panels). Staining for FLAG-tagged Smad7 is shown in green, and that for 6Myc-tagged Smurf1(CA) or WWP1(CA) is shown in red

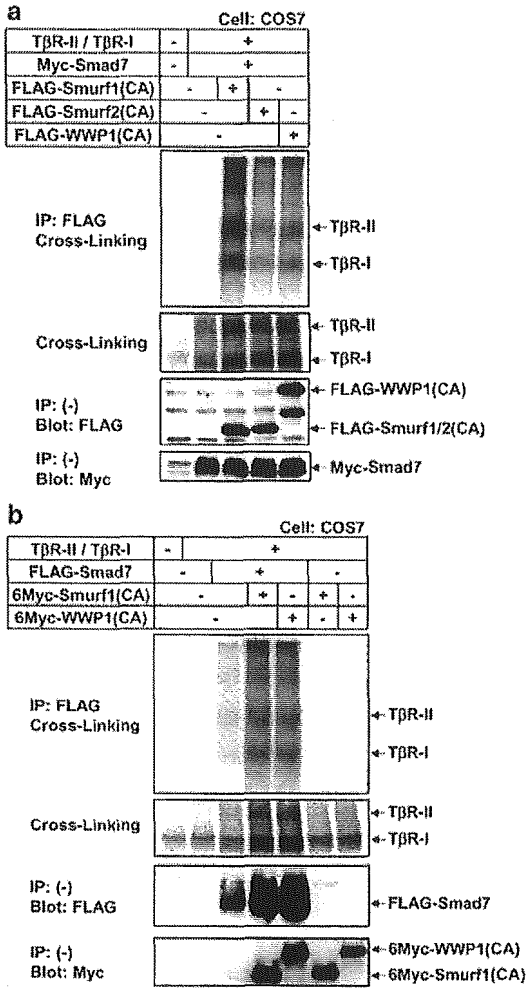

Figure 3 WWP1 interacts with TGF-β receptor complex via Smad7. COS7 cells were transfected with the plasmids indicated. Cells were affinity-labeled with [^{125}I]TGF-β1, followed by immunoprecipitation with anti-FLAG antibody. (**a**) E3 ubiquitin ligases were immunoprecipitated in the presence of Smad7. (**b**) Smad7 was immunoprecipitated in the presence of E3 ligases. Immune complexes were subjected to SDS–PAGE and co-precipitated receptor complexes (top panels) and cell surface receptors (second panels) were analyzed using a Fuji BAS 5000 Bio-imaging Analyzer (Fuji Photo Film). The lower two panels show the expression of each protein analyzed by immunoblotting

TβR-I(TD) was induced by WWP1(WT), but not by WWP1(CA), and the ubiquitination was enhanced in the presence of Smad7. In Figure 4b, we show the results of pulse-chase analysis of the degradation of TβR-I(TD) by Smad7-WWP1 complex. FLAG-tagged TβR-I(TD) proteins were observed as two differentially migrating bands. Since membrane receptors are post-translationally modified by the addition of N-linked oligosaccharides, the slowly migrating bands most likely represent a mature form of TβR-I(TD), whereas the rapidly migrating band represents its immature form. In the presence of Smad7, WWP1(WT) and Smurf1(WT), but not WWP1(CA), accelerated degradation of TβR-I(TD).

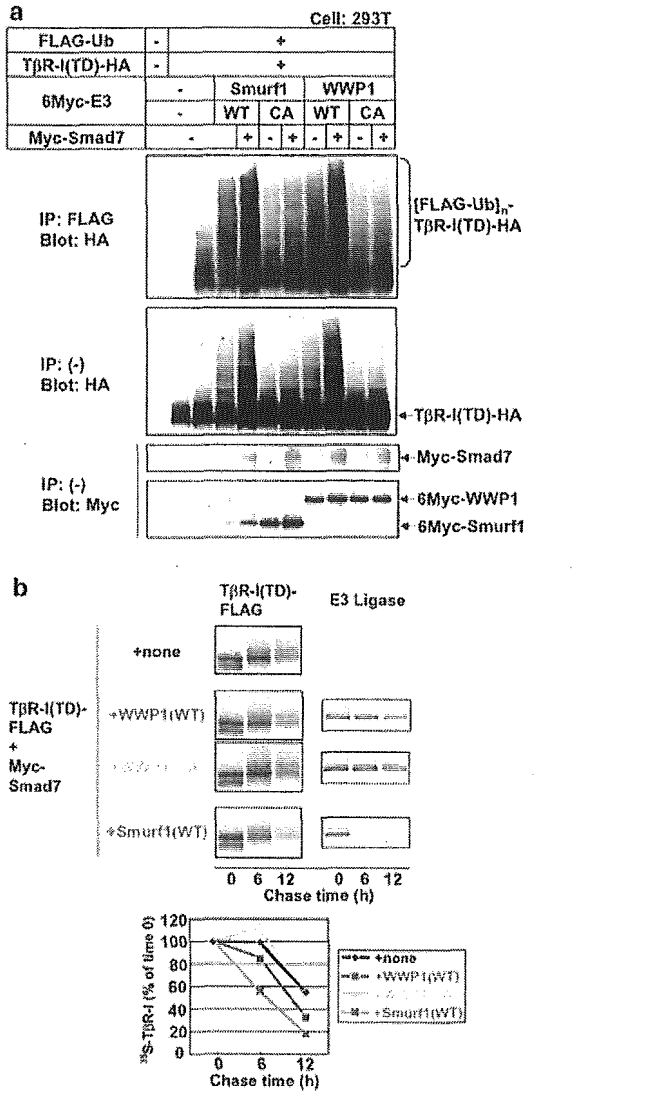

Figure 4 WWP1 induces ubiquitination and degradation of constitutively active TβR-I, TβR-I(TD). (**a**) Ubiquitination of TβR-I(TD) by WWP1. 293T cells were transfected with the plasmids indicated and treated with 2 μM of lactacystin for 24 h before cell lysis. Ubiquitinated proteins were immunoprecipitated from lysates with anti-FLAG antibody followed by anti-HA-immunoblotting. The top panel shows ubiquitination of the receptor, and the lower three panels show the expression of each protein. (**b**) WWP1 induces rapid turnover of TβR-I(TD). COS7 cells were transfected with TβR-I(TD)-FLAG and Myc-Smad7, with or without FLAG-WWP1(WT), FLAG-WWP1(CA), or FLAG-Smurf1(WT) and used for pulse-chase analysis. Total cell lysates were subjected to immunoprecipitation with anti-FLAG antibody and analysed. The autoradiographic signals were quantified and values were plotted relative to the 0-h values

These results suggest that WWP1 interacts with TβR-I via Smad7 and induces ubiquitination and degradation of the receptor.

WWP1 failed to ubiquitinate R-Smad and SnoN

Since WWP1 associates not only with I-Smads but also with TGF-β/BMP-activated Smads 1, 2, 3 and 5

(Figure 1b), we next examined the effect of WWP1 on ubiquitination of Smad proteins. Since Smurf2 induces ubiquitination of Smad2 (Lin *et al.*, 2000), we first compared the effect of Smurf2 on ubiquitination of Smad2 with that of WWP1 in transfected 293T cells. Even in the presence of TβR-I(TD), WWP1(WT) did not induce ubiquitination of Smad2, whereas Smurf2 did so strongly (Figure 5a). We also examined whether WWP1 causes ubiquitination of other Smad proteins. As shown in Figure 5b, WWP1 induced ubiquitination of Smads 6 and 7, but not of other Smads, indicating that WWP1 associates with R-Smads in a ligand-dependent fashion, but fails to induce their ubiquitination.

A previous study showed that Smurf2 associates with SnoN via Smad2 and induces ubiquitin-mediated degradation of SnoN (Bonni *et al.*, 2001). We therefore investigated whether WWP1 acts as an E3 ligase for SnoN. We first tested interaction of WWP1 with SnoN via Smad2. WWP1(CA) bound to SnoN even in the absence of Smad2, and the interaction was enhanced in the presence of both Smad2 and TβR-I(TD) (Figure 6a). We next examined whether WWP1 induces ubiquitination of SnoN. Smurf2 or WWP1 was cotransfected with various combinations of the indicated plasmids into 293T cells. Smurf2 strongly induced ubiquitination of SnoN, whereas WWP1 failed to do so (Figure 6b). These results suggest that, in contrast to Smurf2, WWP1 does not affect the degradation of SnoN, although WWP1 interacts with SnoN.

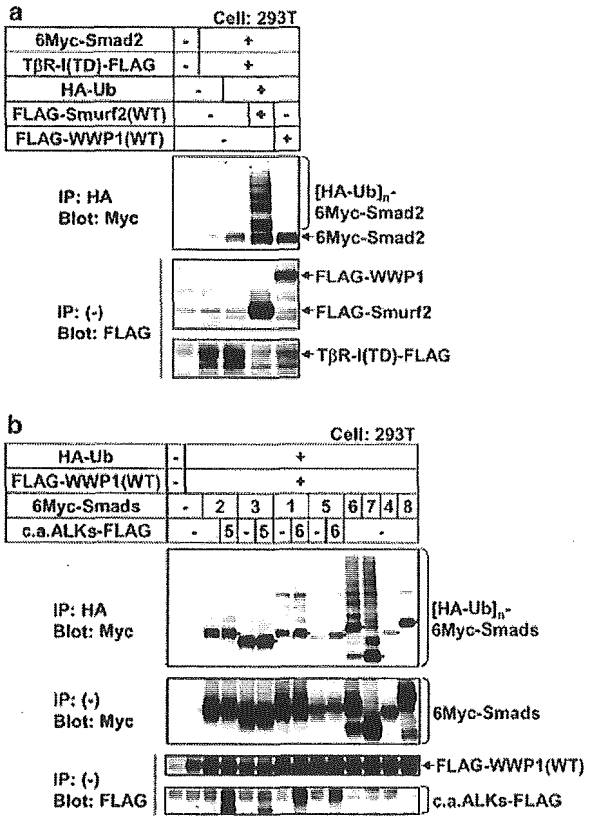

Figure 5 WWP1 fails to induce ubiquitination of R-Smads. (**a**) Effect of WWP1 on ubiquitination of Smad2. 293T cells were transfected with the plasmids indicated and treated with 2 μM of lactacystin for 24 h before cell lysis. Ubiquitinated proteins were immunoprecipitated from cell lysates with anti-HA antibody followed by anti-Myc-immunoblotting. The top panel shows ubiquitination of Smad2, and the lower two panels show the expression of each protein. Note that nonubiquitinated 6Myc-Smad2 was co-precipitated with ubiquitin in the presence of E3 ligases, probably because E3 ligases bridge ubiquitin and Smad2. Ubiquitin itself also has weak interaction with Smad proteins. (**b**) Ubiquitination of Smad proteins by WWP1. The top panel shows ubiquitination of the Smad proteins, and the lower three panels show the expression of each protein. Dots correspond to the position of nonubiquitinated 6Myc-Smads

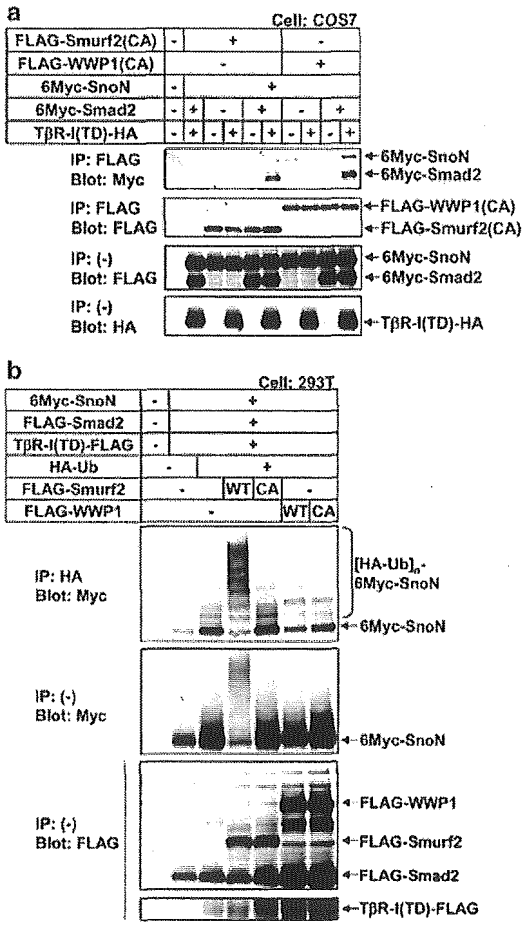

Figure 6 WWP1 fails to induce ubiquitination of SnoN. (**a**) Interaction of WWP1 with SnoN. Binding of WWP1(CA) to SnoN was examined in transfected cells. COS7 cells were transfected with the plasmids indicated. Cell lysates were subjected to immunoprecipitation with anti-FLAG antibody, followed by anti-Myc or anti-FLAG-immunoblotting. The top panel shows the interaction, the second panel monitors immunoprecipitation, and the two bottom panels show the expression of each protein. (**b**) Effects of WWP1 on ubiquitination of SnoN. 293T cells were transfected with the indicated plasmids. Cell lysates were subjected to immunoprecipitation with anti-HA antibody followed by anti-Myc immunoblotting. The top panel shows ubiquitination of SnoN, and the lower three panels show the expression of each protein. The bottom bands in the top panel correspond to nonubiquitinated SnoN that was co-precipitated with HA-ubiquitin

Phosphorylation of Smad2 by TβR-I is inhibited in the presence of WWP1

We next examined the effect of WWP1 on TβR-I-induced phosphorylation of Smad2. In transfected COS7 cells, WWP1 inhibited phosphorylation of Smad2 in a dose-dependent fashion while the protein expression level of Smad2 was constant (Figure 7a). Smurf1 strongly inhibited phosphorylation of Smad2, which was accompanied by a reduction in the Smad2 expression level. WWP1(CA), which lacks ubiquitin ligase activity, failed to inhibit phosphorylation of Smad2 (Figure 7b). These results are consistent with our finding that WWP1 induces ubiquitination and degradation of TβR-I but not of R-Smads.

Endogenous WWP1 negatively regulates Smad signaling

We asked whether endogenous WWP1 is involved in the regulation of TGF-β signaling in cooperation with Smad7. We first examined the interaction of endogenous WWP1 and Smad7. Lysates from HepG2 cells were subjected to immunoprecipitation using anti-WWP1, anti-Smad7, or nonspecific IgG. WWP1 in the precipitates was then visualized by immunoblotting (Figure 8a). WWP1 was precipitated by anti-WWP1 and anti-Smad7, but not by nonspecific IgG.

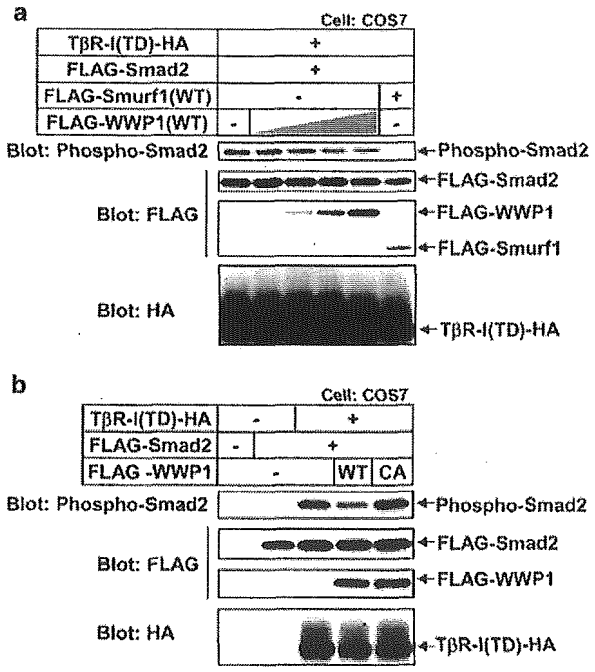

Figure 7 WWP1 inhibits phosphorylation of Smad2 by constitutively active TGF-β type I receptor. The effect of increasing amount of WWP1 on phosphorylation Smad2 by TβR-I(TD) (**a**) as well as the effect of WWP1(CA) (**b**) was examined. COS7 cells were transfected with the plasmids indicated. cDNAs were transfected at the doses of 0.05, 0.1, 0.2 and 0.4 μg (WWP1(WT)), 0.4 μg (WWP1(CA)), and 0.4 μg. (Smurf1(WT)). The top panel shows phosphorylation Smad2 by anti-phospho-Smad2 immunoblotting, and the lower three panels show the expression of each protein as indicated

We next examined the effect of suppression of WWP1 by siRNA on TGF-β signaling. The efficiency of the siRNA was confirmed by the reduction of WWP1 expression in transfected 293T cells (Figure 8b). TGF-β-responsive reporter activity was significantly enhanced in the presence of siRNA specific for WWP1 in 293 cells (Figure 8c). Similar results were obtained when we used HeLa cells and MCF-7 cells (data not shown). These data support the conclusion that WWP1 functions as a negative regulator of TGF-β signaling.

Expression of WWP1 mRNA in various human tissues and carcinoma cell lines

We examined the expression levels of WWP1 mRNA in various human tissues by quantitative real-time PCR and compared the expression profile with that of Smurf1 (Figure 9a). Both WWP1 and Smurf1 were widely expressed, but exhibited distinct tissue distribution. Smurf1 was highly expressed in testis, and moderately expressed in placenta and pancreas. WWP1 was highly

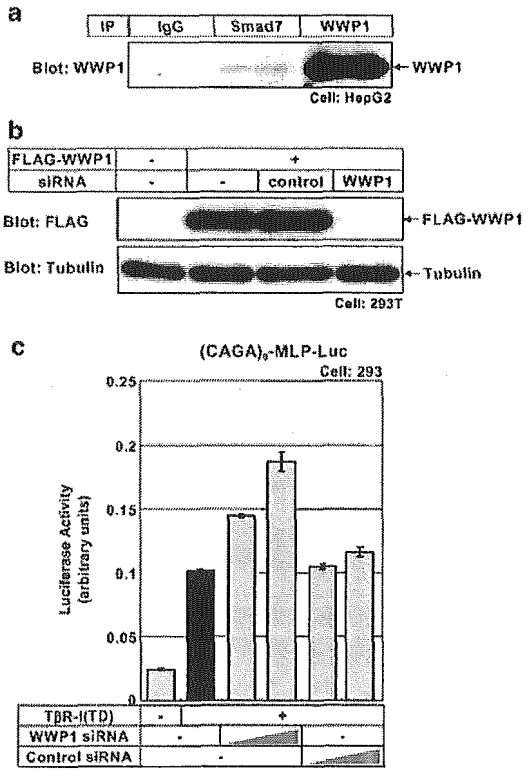

Figure 8 Endogenous WWP1 negatively regulates Smad signaling. (**a**) Interaction of endogenous WWP1 and Smad7. Immunoprecipitation using nonspecific IgG, anti-Smad7, or anti-WWP1 was performed from cell lysate of HepG2, and precipitated WWP1 was visualized by immunoblotting using anti-WWP1. (**b**) Confirmation of siRNA. Expression level of WWP1 in the presence of control or WWP1 siRNA was determined by immunoblotting using transfected 293T cells. (**c**) Effect of the WWP1 siRNA on TGF-β-induced transcriptional activation. Luciferase reporter assay using $(CAGA)_9$-MLP-Luc was performed in 293 cells in the presence of control or WWP1 siRNA

expressed in liver, and moderately expressed in several tissues including heart, placenta, skeletal muscle, kidney, pancreas, and testis. In heart, liver, skeletal muscle, and kidney where WWP1 was highly or moderately expressed, Smurf1 was expressed in only low amounts. These results suggest that signaling of TGF-β in various tissues is differently regulated by HECT-type E3 ubiquitin ligases including Smurfs and WWP1.

We also examined the expression levels of WWP1 and Smurfs in normal cells as well as carcinoma cell lines of human origin (Figure 9b). WWP1 expression was upregulated in several carcinoma cell lines including HT29, MKN-7, MKN-74, MCF-7, and OVCAR-5.

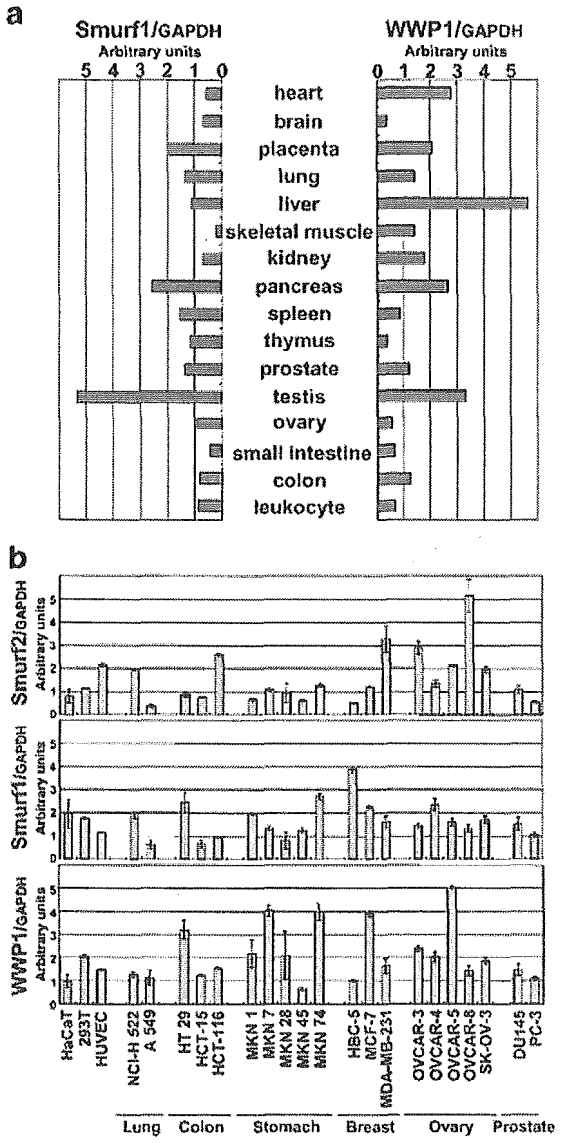

Figure 9 Expression of WWP1 mRNA in various human tissues (**a**) and carcinoma cell lines (**b**). The expression levels of mRNA for WWP1 and Smurfs were examined by real-time PCR, and quantitated values were normalized by the amount of GAPDH mRNA, and results are given as arbitrary units. HaCaT cells, 293T cells, and HUVEC are used as normal cell controls

Expression of Smurf2 was also higher in several carcinoma cell lines including HCT-116, MDA-MB-231, OVCAR-3, and OVCAR-8. In contrast, there was no marked difference in expression levels of Smurf1 among cells examined except HBC-5.

Discussion

TGF-β inhibits growth of various types of cells, and many carcinoma cell lines were found to be resistant to the growth inhibitory activity of TGF-β (Fynan and Reiss, 1993). Thus, inactivation of TGF-β signaling pathway as well as enhancement of expression of the signaling inhibitors may contribute to tumor progression (Massagué *et al*., 2000). Recently, TGF-β signaling inhibitors Smad7 and Smurf2 have been reported to be overexpressed in some types of cancer (Kleeff *et al*., 1999; Fukuchi *et al*., 2002). In the present study, we performed yeast two-hybrid screening to search for novel TGF-β signaling regulators, and identified WWP1 as a Smad7 binding protein that inhibits TGF-β signaling.

WWP1 inhibited transcriptional activity induced by TGF-β type I receptor. Although WWP1 has been reported to suppress activity of transcriptional activator LKLF (Conkright *et al*., 2001), it appears to inhibit TGF-β signaling not at the transcriptional level but rather through downregulation of TGF-β type I receptor function. Like Smurfs, WWP1 associated with Smad7 and induced nuclear export of Smad7. Moreover, WWP1 interacted with TGF-β receptor complex via Smad7, and induced ubiquitination and degradation of the TGF-β type I receptor. Consistent with these results, WWP1(WT), but not WWP1(CA), inhibited phosphorylation of Smad2 by the receptor.Thus, WWP1 acts as an E3 ubiquitin ligase of TGF-β type I receptor to inhibit TGF-β signaling.

We previously reported that Smurf1 negatively regulates TGF-β signaling as well as BMP signaling in cooperation with I-Smads (Murakami *et al*., 2003). Similarly, WWP1 represses transcriptional activity induced by constitutively active BMP-type IB receptor (unpublished observation). WWP1 probably binds to the BMP receptor via I-Smads, thereby antagonizing BMP signaling.

Several characteristics of WWP1, however, differ from those of Smurfs. In transfected mammalian cells, WWP1 and Smurfs interacted not only with Smad7 but also with other Smads, including Smads 1, 2, 3, 5, and 6 (Figure 2a). Smurf1 has been shown to ubiquitinate Smad1, 5, and 6 (Zhu *et al*., 1999; Murakami *et al*., 2003), and Smurf2 has been shown to ubiquitinate Smad1 and 2 (Lin *et al*., 2000; Zhang *et al*., 2001). In contrast, WWP1 induced ubiquitination of Smads 6 and 7, but not of other Smads. These results suggested that WWP1 associates with R-Smads but fails to induce their ubiquitination. It will be important to determine factor(s) permitting ubiquitination of R-Smads by Smurf-like E3 ubiquitin ligases. It has been reported

that association of HECT-type E3 ligases with their potential target proteins is not sufficient to induce ubiquitination (Schwarz *et al.*, 1998). Although Smurfs as well as WWP1 bind to Smad proteins through the interaction of their WW domains with PY motifs on Smad proteins, HECT domains may also contribute to defining the substrate specificity. Alternatively, relative orientation of substrate-binding WW domains and HECT domain in each E3 ligases may affect specificity in ubiquitination of Smad proteins.

Recently, Bonni *et al.* (2001) reported that Smurf2 associates with SnoN via Smad2, and induces ubiquitin-mediated degradation of SnoN, but not that of Smad2. SnoN is a transcriptional corepressor that interacts with Smad2/3 and Smad4, and represses TGF-β signaling (Stroschein *et al.*, 1999). Thus, Smurf2 is thought to enhance TGF-β signals under certain conditions. In the present study, we found that WWP1 failed to induce ubiquitin-mediated degradation of SnoN, although WWP1 bound strongly to SnoN via Smad2 (Figure 6), suggesting that WWP1 functions through similar, but distinct, mechanisms to Smurfs.

In addition to the mechanism of action, WWP1 and Smurfs have different expression profiles. We examined the expression levels of WWP1 mRNA in various human tissues and compared the expression profile with that of Smurf1 (Figure 8a). WWP1 and Smurf1 are widely expressed but exhibited distinct tissue distribution, suggesting the tissue-specific role of WWP1 and Smurfs in negative regulation of TGF-β superfamily signaling. It is interesting to note that the half-life of WWP1 protein was much longer than that of Smurf1 protein in the pulse-chase experiment (Figure 4b). Expression of Smurfs was upregulated in response to TGF-β as well as BMP, whereas expression of WWP1 was not significantly altered (unpublished observations). Taken together, Smurfs appear to have a dynamic role in regulation of TGF-β superfamily signaling, whereas WWP1 may be constitutively and stably expressed in cells and determine the basal level of cellular response to TGF-β superfamily ligands. In this respect, it is noteworthy that WWP1 is overexpressed in several carcinoma cell lines including TGF-β-resistant HT-29 and MCF-7 cells (Arteaga *et al.*, 1988; Li *et al.*, 1995) (Figure 8b). It raises the possibility that overexpression of WWP1 results in resistance to growth inhibition by TGF-β, which may lead to tumor progression.

Although WWP1 and Smurfs blocked TGF-β and BMP signaling, the inhibitory activity of WWP1 was lower than that of Smurfs. There are two possible explanations for this. First, Smurfs induce ubiquitin-dependent degradation of R-Smads to inhibit TGF-β signaling, whereas WWP1 does not. Second, WWP1 has a lower ligase activity to the receptors than that of Smurfs.

In conclusion, we identified WWP1 as a new member of the Smurf-like C2-WW-HECT-type E3 ubiquitin ligases that negatively regulates TGF-β superfamily signaling. Like Smurf1 and 2, WWP1 induces ubiquitin-dependent degradation of TβR-I, whereas it fails to degrade R-Smads and SnoN. Importantly, WWP1 and Smurfs are expressed in distinct patterns in human tissues and carcinoma cell lines. It will be important to determine in the future how the expression and the function of WWP1 are regulated under pathological conditions.

Materials and methods

Yeast two-hybrid screening

To construct a bait plasmid, full-length mouse Smad7 cDNA was inserted in-frame into pGBKT7 GAL4 DNA-binding vector. This construct was introduced into the yeast strain AH109 and used to screen a human lung cDNA library in the pGAD vector (Clontech) on synthetic defined medium that was deficient in leucine, tryptophan, histidine, and adenine (SD-L-W-A-H) with 3-AT 3 mM. Library plasmids were rescued from the yeast and sequenced.

DNA construction and transfection

The original constructions of constitutively active forms of TGF-β type I and BMP type IB receptors (TβR-I(TD) and BMP-IB(QD), respectively), Smad1-8, and Smurf1 and 2 were described previously (Kawabata *et al.*, 1998; Ebisawa *et al.*, 2001; Suzuki *et al.*, 2002). The open reading frame of WWP1 was generated by a polymerase chain reaction (PCR)-based approach using an EST clone of WWP1 (GenBank accession no. BI560015, ResGen) as a template, and subcloned into *Eco*RI/*Xho*I-digested FLAG-pcDNA3 (Kawabata *et al.*, 1998). The catalytically inactive form of WWP1 (WWP1(CA)), in which cysteine 890 was replaced with alanine, was generated by a PCR-based approach. COS7 cells, 293T cells, HeLa cells, HepG2 cells, and R mutant mink lung epithelial (Mv1Lu) cells were transiently transfected using FuGENE6 (Roche Diagnostics) as previously described (Kawabata *et al.*, 1998).

Luciferase assay

HepG2 cells, R mutant Mv1Lu cells, or HEK293 cells were transiently transfected with an appropriate combination of promoter–reporter constructs, expression plasmids, and pcDNA3. At 24 h after transfection, cell lysates were prepared, and luciferase activity was measured by the Dual-Luciferase Reporter System (Promega) as previously described (Hanyu *et al.*, 2001). Values were normalized using Renilla luciferase activity under control of CMV promoter.

Immunoprecipitation and immunoblotting

Cells were lysed with Nonidet P-40 lysis buffer (20 mM Tris-HCl, pH 7.5, 150 mM NaCl, 1% Nonidet P-40). Immunoprecipitation and immunoblotting were performed as described previously (Kawabata *et al.*, 1998). For inhibition of proteasomal degradation, cells were incubated with 2 μM of lactacystin (Calbiochem) for 24 h before cell lysis, unless otherwise indicated. Antibodies used were anti-FLAG M2 (Sigma), anti-Myc 9E10 (Pharmingen), anti-HA 12CA5 (for immunoprecipitation) or 3F10 (for immunoblotting) (Roche Diagnostics), anti-phospho-Smad2 (Cell Signaling), anti-WWP1 (Santa Cruz, sc-11893), and anti-Smad7 (Koinuma *et al.*, 2003).

Immunofluorescence labeling

Immunocytochemical staining of FLAG-Smad7, 6Myc-Smurf1(CA), or 6Myc-WWP1(CA) in transfected HeLa cells

was performed using mouse anti-FLAG or anti-Myc antibody followed by incubation with fluorescein isothiocyanate (FITC)-labeled goat anti-mouse IgG as previously described (Ebisawa *et al.*, 2001). For double staining of FLAG-Smad7 and 6Myc-E3 ubiquitin ligase, mouse anti-FLAG and rabbit anti-Myc antibodies were used and detected with FITC-labeled goat anti-mouse IgG or rhodamine isothiocyanate (RITC)-labeled goat anti-rabbit IgG, respectively. Cell nuclei were stained by propidium iodide (PI). Intracellular localization was determined by confocal laser scanning microscopy.

Affinity crosslinking and immunoprecipitation

Recombinant TGF-β1 (R&D Systems) was iodinated using the chloramine T method as described previously (Frolik *et al.*, 1984). The immunoprecipitation of the crosslinked complex and analysis by SDS–polyacrylamide gel electrophoresis (PAGE) were performed as described previously (Ebisawa *et al.*, 1999).

Pulse-chase analysis

Transfected COS7 cells were labeled for 10 min at 37°C with 50 μCi/ml [^{35}S]methionine and cysteine (Amersham Biosciences) in methionine- and cysteine-free Dulbecco's modified Eagle's medium (DMEM) and chased in DMEM supplemented with 0.2% fetal bovine serum and unlabeled methionine and cysteine for the time periods indicated as previously described (Ebisawa *et al.*, 2001). Cells were then lysed and the protein extracts were subjected to immunoprecipitation followed by SDS–PAGE. The gels were fixed, dried, and protein bands were visualized using a Fuji BAS 5000 Bio-Imaging Analyzer (Fuji Photo Film).

RNA interference

RNA interference was performed as described by Brummelkamp *et al.* (2002). HEK293 cells were transfected with pSUPER vectors using FuGENE6 (Roche Applied Science). To generate WWP1-pSUPER, oligonucleotides (forward: 5′-gatccccGAGTTGATGATCGTAGAAGttcaagagaCTTCTACGATCATCAACTCtttttggaaa-3′; reverse: 5′-agcttttccaaaaa-GAGTTGATGATCGTAGAAGtctcttgaaCTTCTACGAT-CATCAACTCggg-3′) were annealed, followed by ligation into the pSUPER vector, which was digested with *Bgl*II/*Hind*III. NC1-pSUPER (negative control) was described previously (Maeda *et al.*, 2004). To confirm the knockdown of WWP1, 293T cells were transfected with WWP1 cDNA (FLAG-tagged construct, 0.3 μg) and siRNA pSUPER constructs (NC1 and WWP1; 0.05 and 0.1 μg). Expression level of WWP1 protein was then determined by immunoblotting using anti-FLAG (M2) antibody. Luciferase reporter assay using $(CAGA)_9$-MLP-Luc was performed in the presence of pSUPER constructs (NC1 and WWP1; 0.05 and 0.1 μg).

Real-time PCR

Quantitative real-time PCR analysis was performed using the ABI PRISM 7000 Sequence Detection System (Applied Biosystems). The cDNA templates from various human tissues were purchased from BD Biosciences (Human MTC Panel I/II), and those from HaCaT cells, 293T cells, HUVECs, and human carcinoma cell lines were described previously (Dan *et al.*, 2002; Ota *et al.*, 2002; Koinuma *et al.*, 2003). The primer sequences used were as follows: human WWP1: forward, 5′-GTA TGG ATC CTG TAC GGC AGC A, reverse, 5′-GTT GTG GTC TCT CCC ATG TGG T, human Smurf1: forward, 5′-GTC CAG AAG CTG AAA GTC CTC AGA, reverse, 5′-CAC GGA ATT TCA CCA TCA GCC, human Smurf2: forward, 5′-GGC AGA ACC AAT TGA AAG ACC A, reverse, 5′-GTT TCT GAA CAA GGT CTC GCT T, human GAPDH: forward, 5′-GAA GGT GAA GGT CGG AGT C, reverse, 5′-GAA GAT GGT GAT GGG ATT TC.

Acknowledgements
We are grateful to Yuri Inada and Aki Hanyu, Ken Shirakawa for technical help. This study was supported by Grants-in-Aid for Scientific Research from the Ministry of Education, Culture, Sport, Science, and Technology of Japan, and by the Viral Hepatitis Research Foundation of Japan.

References

Arteaga CL, Tandon AK, Von Hoff DD and Osborne CK. (1988). *Cancer Res.*, **48,** 3898–3904.
Attisano L and Wrana JL. (2000). *Curr. Opin. Cell. Biol.*, **12,** 235–243.
Bonni S, Wang HR, Causing CG, Kavsak P, Stroschein SL, Luo K and Wrana JL. (2001). *Nat. Cell Biol.*, **3,** 587–595.
Brummelkamp TR, Bernards R and Agami R. (2002). *Science*, **296,** 550–553.
Conkright MD, Wani MA and Lingre JB. (2001). *J. Biol. Chem.*, **276,** 29299–29306.
Dan S, Tsunoda T, Kitahara O, Yanagawa R, Zembutsu H, Katagiri T, Yamazaki K, Nakamura Y and Yamori T. (2002). *Cancer Res.*, **62,** 1139–1147.
Derynck R, Zhang Y and Feng X-H. (1998). *Cell*, **95,** 737–740.
Ebisawa T, Fukuchi M, Murakami G, Chiba T, Tanaka K, Imamura T and Miyazono K. (2001). *J. Biol. Chem.*, **276,** 12477–12480.
Ebisawa T, Tada K, Kitajima I, Tojo K, Sampath TK, Kawabata M, Miyazono K and Imamura T. (1999). *J. Cell Sci.*, **112,** 3519–3527.
Flasza M, Gorman P, Roylance R, Canfield AE and Baron M. (2002). *Biochem. Biophys. Res. Commun.*, **290,** 431–437.
Frolik CA, Wakefield LM, Smith DM and Sporn MB. (1984). *J. Biol. Chem.*, **259,** 10995–11000.
Fukuchi M, Fukai Y, Masuda N, Miyazaki T, Nakajima M, Sohda M, Manda R, Tsukada K, Kato H and Kuwano H. (2002). *Cancer Res.*, **62,** 7162–7165.
Fynan TM and Reiss M. (1993). *Crit. Rev. Oncol.*, **4,** 493–540.
Hanyu A, Ishidou Y, Ebisawa T, Shimanuki T, Imamura T and Miyazono K. (2001). *J. Cell Biol.*, **155,** 1017–1028.
Heldin C-H, Miyazono K and ten Dijke P. (1997). *Nature*, **390,** 465–471.
Huang K, Johnson KD, Petcherski AG, Vandergon T, Mosser EA, Copeland NG, Jenkins NA, Kimble J and Bresnick EH. (2000). *Gene*, **252,** 137–145.
Imamura T, Takase M, Nishihara A, Oeda E, Hanai J, Kawabata M and Miyazono K. (1997). *Nature*, **389,** 622–626.
Kavsak P, Rasmussen RK, Causing CG, Bonni S, Zhu H, Thomsen GH and Wrana JL. (2000). *Mol. Cell*, **6,** 1365–1375.
Kawabata M, Inoue H, Hanyu A, Imamura T and Miyazono K. (1998). *EMBO J.*, **17,** 4056–4065.

Kleeff J, Ishiwata T, Maruyama H, Friess H, Truong P, Buchler MW, Falb D and Korc M. (1999). *Oncogene*, **18,** 5363–5372.
Koinuma D, Shinozaki M, Komuro A, Goto K, Saitoh M, Hanyu A, Ebina M, Nukiwa T, Miyazawa K, Imamura T and Miyazono K. (2003). *EMBO J.*, **22,** 1–13.
Li CY, Suardet L and Little JB. (1995). *J. Biol. Chem.*, **270,** 4971–4974.
Lin X, Liang M and Feng X-H. (2000). *J. Biol. Chem.*, **275,** 36818–36822.
Maeda S, Hayashi M, Komiya S, Imamura T and Miyazono K. (2004). *EMBO J.*, **23,** 552–563.
Massagué J, Blain SW and Lo RS. (2000). *Cell*, **103,** 295–309.
Miyazawa K, Shinozaki M, Hara T, Furuya T and Miyazono K. (2002). *Genes Cells*, **7,** 1191–1204.
Murakami G, Watabe T, Takaoka K, Miyazono K and Imamura T. (2003). *Mol. Biol. Cell*, **14,** 2809–2817.
Ota T, Fujii M, Sugizaki T, Ishii M, Miyazawa K, Aburatani H and Miyazono K. (2002). *J. Cell. Physiol.*, **193,** 299–318.
Pirozzi G, McConnell SJ, Uveges AJ, Carter JM, Sparks AB, Kay BK and Fowlkes DM. (1997). *J. Biol. Chem.*, **272,** 14611–14616.
Roberts AB and Sporn MB. (1990) In Sporn MB and Roberts AB (eds). *Peptide Growth Factors and Their Receptors, Part I.* Springer-Verlag: Heidelberg, pp. 419–472.
Schwarz SE, Rosa JL and Scheffner M. (1998). *J. Biol. Chem.*, **273,** 12148–12154.
Stroschein SL, Wang W, Zhou S, Zhou Q and Luo K. (1999). *Science*, **286,** 771–774.
Suzuki C, Murakami G, Fukuchi M, Shimanuki T, Shikauchi Y, Imamura T and Miyazono K. (2002). *J. Biol. Chem.*, **277,** 39919–39925.
Tajima Y, Goto K, Yoshida M, Shinomiya K, Sekimoto T, Yoneda Y, Miyazono K and Imamura T. (2003). *J. Biol. Chem.*, **278,** 10716–10721.
Zhang Y, Chang C, Gehling DJ, Hemmati-Brivanlou A and Derynck R. (2001). *Proc. Natl. Acad. Sci. USA*, **98,** 974–979.
Zhu H, Kavsak P, Abodollah S, Wrana JL and Thomsen GH. (1999). *Nature*, **400,** 687–693.

THE JOURNAL OF BIOLOGICAL CHEMISTRY
Vol. 279, No. 17, Issue of April 23, pp. 17634–17639, 2004
Printed in U.S.A.

Lysophosphatidic Acid and Autotaxin Stimulate Cell Motility of Neoplastic and Non-neoplastic Cells through LPA_1*

Received for publication, December 19, 2003, and in revised form, January 20, 2004
Published, JBC Papers in Press, January 26, 2004, DOI 10.1074/jbc.M313927200

Kotaro Hama‡, Junken Aoki‡§, Masahiro Fukaya¶, Yasuhiro Kishi‡, Teruyuki Sakai‖, Rika Suzuki‖, Hideo Ohta‖, Takao Yamori, Masahiko Watanabe¶, Jerold Chun‡‡, and Hiroyuki Arai‡**

*From the ‡Graduate School of Pharmaceutical Sciences, The University of Tokyo, 7-3-1, Hongo, Bunkyo-ku, Tokyo 113-0033, Japan, the ¶Department of Anatomy, Hokkaido University School of Medicine, Sapporo 060-8638, Japan, the ‖Pharmaceutical Research Laboratory, Kirin Brewery Company Ltd., 3 Miyahara, Takasaki, Gunma 370-1295, Japan, the **Division of Molecular Pharmacology, Cancer Chemotherapy Center, Japanese Foundation for Cancer Research, Toshima-ku, Tokyo 170-8455, Japan, and the ‡‡Department of Molecular Biology, The Scripps Research Institute, La Jolla, California 92037*

Autotaxin (ATX) is a tumor cell motility-stimulating factor originally isolated from melanoma cell supernatant that has been implicated in regulation of invasive and metastatic properties of cancer cells. Recently, we showed that ATX is identical to lysophospholipase D, which converts lysophosphatidylcholine to a potent bioactive phospholipid mediator, lysophosphatidic acid (LPA), raising the possibility that autocrine or paracrine production of LPA by ATX contributes to tumor cell motility. Here we demonstrate that LPA and ATX mediate cell motility-stimulating activity through the LPA receptor, LPA_1. In fibroblasts isolated from $lpa_1^{-/-}$ mice, but not from wild-type or $lpa_2^{-/-}$, cell motility stimulated with LPA and ATX was completely absent. In the $lpa_1^{-/-}$ cells, LPA-stimulated lamellipodia formation was markedly diminished with a concomitant decrease in Rac1 activation. LPA stimulated the motility of multiple human cancer cell lines expressing LPA_1, and the motility was attenuated by an LPA_1-selective antagonist, Ki16425. The present study suggests that ATX and LPA_1 represent potential targets for cancer therapy.

Cell migration is an important cellular function for many physiological processes, such as embryonic morphogenesis, wound healing, immune-cell trafficking, and brain development (1). In addition to physiological functions, cancer cells use migration mechanisms that are similar to those that occur in non-neoplastic cells (2). The principles of cell migration were initially investigated in non-neoplastic fibroblasts, keratinocytes, and myoblasts, and additional studies on tumor cells identified the same basic mechanisms. Understanding more about the cellular and molecular basis of different cell migration/invasion mechanisms will help us to explain how cancer cells disseminate and should lead to new treatment strategies.

Lysophosphatidic acid (LPA)[1] (1- or 2-acyl-*sn*-glycerol-3-phosphate) is a naturally occurring phospholipid. It evokes a variety of biological responses, including platelet aggregation, smooth-muscle contraction, neurite retraction, and cell proliferation (3, 4). LPA stimulates cell migration in many cell types *in vitro*, including fibroblasts, gliomas, T lymphomas, and colorectal cancer cells (5–7), indicating a potential role of LPA in cellular migration in both physiological and pathological conditions (8). A role for LPA signaling in cancer cell migration received further support from the identification of autotaxin (ATX), a protein previously implicated in neoplastic invasion and metastasis (9), as a major biosynthetic enzyme for LPA. ATX was found to be identical to lysophospholipase D, an LPA-producing enzyme in blood that converts lysophosphatidylcholine to LPA (10, 11). ATX also shows properties of a nucleotide pyrophosphatase/phosphodiesterase, which might also explain its bioactivities. It has been shown that LPA- and ATX-stimulated cell motility is attenuated by treating cells with pertussis toxin (PTX) (8, 12–13), suggesting that G protein-coupled receptors (GPCRs) coupled with $G_{i/o}$ are involved. LPA elicits most of the cellular events via signal transduction cascades downstream of its specific GPCRs, LPA_1/Edg-2, LPA_2/Edg-4, LPA_3/Edg-7, which belong to the Edg (endothelial cell differentiation gene) family, and LPA_4/GPR23, a non-Edg family LPA receptor (4, 14–17). Non-GPCR pathways have also been proposed (18, 19). Several experiments have demonstrated that these GPCRs can mediate mitogen-activated protein kinase activation, phospholipase C activation, and calcium mobilization through PTX-sensitive ($G_{i/o}$) and -insensitive G proteins ($G_{12/13}$ and $G_{q/11/14}$) (4). However, the LPA receptor subtype involved in LPA-induced cell motility remained to be identified.

In this study, we explored the role of each LPA receptor in LPA- and ATX-induced cell migration. Our results clearly indicate that LPA- and ATX-induced cell motility is driven by LPA_1 activation. We also suggest a crucial role of Rac1 activation in LPA_1-mediated cell migration.

EXPERIMENTAL PROCEDURES

Reagents—1-oleoyl-LPA (18:1) was purchased from Avanti Polar Lipids Inc. (Alabaster, AL). Other chemicals were purchased from Sigma. Recombinant ATX/lysophospholipase D protein was prepared as described previously (10).

Cell Culture—Mouse skin fibroblast (MSF) cells were prepared from skin of newborn mice generated by wild-type or knock-out ($lpa_1^{-/-}$ single, $lpa_2^{-/-}$ single, and $lpa_1^{-/-}lpa_2^{-/-}$ double) intercrosses as described previously (20). MSF cells were cultured in minimum essential medium (Sigma) supplemented with 10% fetal bovine serum, and cells from the first to the fifth passages were used for all experiments. All

* This work was supported in part by research grants from the Ministry of Education, Culture, Sports, Science, and Technology and the Human Frontier Special Program. The costs of publication of this article were defrayed in part by the payment of page charges. This article must therefore be hereby marked "*advertisement*" in accordance with 18 U.S.C. Section 1734 solely to indicate this fact.

§ To whom correspondence should be addressed. Tel.: 81-3-5842-4723; Fax: 81-3-3818-3173; E-mail: jaoki@mol.f.u-tokyo.ac.jp.

[1] The abbreviations used are: LPA, lysophosphatidic acid; ATX, autotaxin; OMPT, 1-oleoyl-2-*O*-methyl-*rac*-glycerophosphothionate; PTX, pertussis toxin; MSF, mouse skin fibroblast; GAPDH, glyceraldehyde-phosphate dehydrogenase; Edg, endothelial cell differentiation gene; GST, glutathione *S*-transferase.

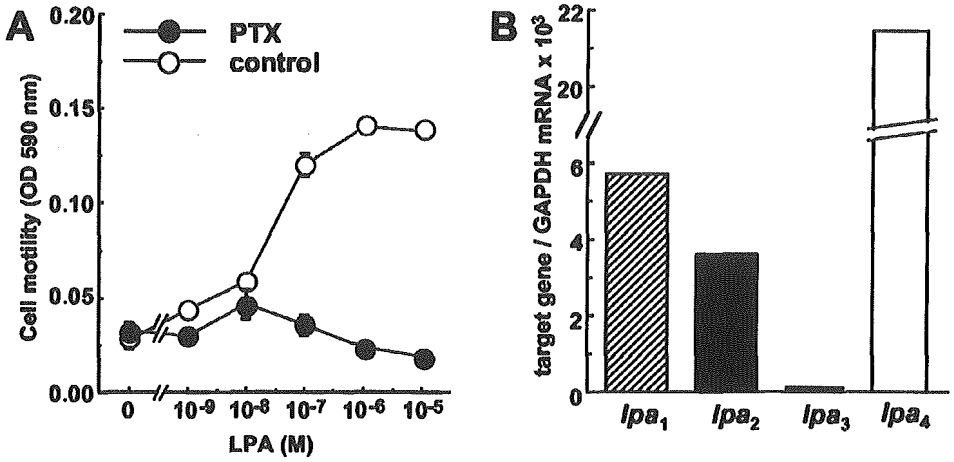

FIG. 1. **LPA induces PTX-sensitive cell motility in mouse skin fibroblasts.** *A*, LPA stimulates cell motility of MSF cells in a PTX-sensitive manner. MSF cells were pretreated with PTX (100 ng ml^{-1}, 24 h), and LPA-induced cell motility was evaluated using the Boyden chamber assay. *B*, expression of each LPA receptor mRNA in MSF cells. The level of LPA receptor mRNA in MSF cells was measured using quantitative real-time RT-PCR and is expressed as a relative value to GAPDH mRNA.

cancer cell lines used in this study were cultured in RPMI 1640 (Sigma) supplemented with 5% fetal bovine serum as described previously (21).

Chemotaxis Assay—Cell migration was measured in a modified Boyden chamber as described previously (10). In brief, polycarbonate filters with 5-μm (MSF cells) or 8-μm pores (carcinoma cell lines) (Neuro Probe, Inc., Gaithersburg, MD) were coated with 0.001% of fibronectin (Sigma). Cells (1×10^5 cells in 200 μl/well) were loaded into upper chambers and incubated at 37 °C for 3 h to allow migration. The cell migration to the bottom side of the filter was evaluated by measuring optical densities at 590 nm. For PTX and Ki16425 treatment, cells were preincubated with 10 ng ml^{-1} of PTX for 24 h and 1 μM Ki16425 for 30 min, respectively.

Quantitative Real-time RT-PCR—Total RNA from cells was extracted using ISOGEN (Nippongene, Toyama, Japan) and reverse-transcribed using the SuperScript first-strand synthesis system for RT-PCR (Invitrogen). Oligonucleotide primers for PCR were designed using Primer Express Software (Applied Biosystems, Foster City, CA). The sequences of the oligonucleotides used in PCR reaction were as follows. LPA_1 (mouse)-forward gaggaatcgggacaccatgat; LPA_1 (mouse)-reverse acatccagcaataacaagaccaatc; LPA_1 (human)-forward aatcgggataccatgatgagtctt; LPA_1 (human)-reverse ccaggagtccagcagatgataaa; LPA_2 (mouse)-forward gaccacactcagcctagtcaagac; LPA_2 (mouse)-reverse cttacagtccaggccatcca; LPA_2 (human)-forward cgctcagcctggtcaagact; LPA_2 (human)-reverse ttgcaggactcacagcctaaac; LPA_3 (mouse)-forward gctcccatgaagctaatgaagaca; LPA_3 (mouse)-reverse aggccgtccagcagcaga; LPA_3 (human)-forward aggacacccatgaagctaatgaa; LPA_3 (human)-reverse gccgtcgaggagcagaac. LPA_4 (mouse)-forward cagtgcctccctgtttgtcttc; LPA_4 (mouse)-reverse gagagggccaggttggtgat. LPA_4 (human)-forward cctagtcctcagtggcggtatt; LPA_4 (human)-reverse ccttcaaagcaggtggtggtt. GAPDH (mouse/human)-forward gccaaggtcatccatgacaact; GAPDH (mouse/human)-reverse gaggggccatccacagtctt. PCR reactions were performed using an ABI Prism 7000 sequence detection system (Applied Biosystems). The transcript number of mouse GAPDH was quantified, and each sample was normalized on the basis of GAPDH content.

Intracellular Calcium Mobilization—A-2058 cells were incubated with 5 μM fura-2 acetoxymethyl ester (Dojin, Tokyo, Japan) in calcium ringer buffer (150 mM NaCl, 4 mM KCl, 2 mM $CaCl_2$, 1 mM $MgCl_2$, 5.6 mM glucose, 0.1% bovine serum albumin, and 5 mM HEPES, pH 7.4) at 37 °C for 30 min. Following stimulation with LPA, cytosolic calcium was measured by monitoring fluorescence intensity at an emission wavelength of 500 nm and excitation wavelengths of 340 and 380 nm using a CAF-110 (JACS, Tokyo, Japan).

Fluorescence Microscopy—MSF cells were seeded onto glass coverslips, grown in the presence of serum to subconfluence, and starved for 24 h by replacing the medium with serum-free medium containing 0.1% bovine serum albumin. Then the cells were treated with 1 μM LPA in serum-free medium for 3 h and stained for F-actin with BODIPY FL phallacidin (Molecular Probes, Inc., Eugene, OR) according to the manufacture's protocol.

Rac1 and RhoA Activity Assays—Measurement of Rac1 and RhoA activities was performed as described previously (22). Cells starved for 24 h were stimulated with LPA (1 μM) and lysed for 5 min in ice-cold cell lysis buffer containing GST-αPAK or GST-Rhotekin. The cell lysates were incubated with glutathione-Sepharose 4B (Amersham Biosciences) for 60 min at 4 °C. After the beads had been washed with the cell lysis buffer, the bound proteins were analyzed by Western blotting using anti-Rac1 antibody (BD Biosciences) or anti-RhoA antibody (Santa Cruz Biotechnology).

RESULTS

To determine whether LPA receptors are required for LPA-dependent cell motility and, if so, which receptor subtype and signaling cascade are utilized, we generated MSF cells isolated from newborn mice. The MSF cells expressed LPA_1, LPA_2, and LPA_4 with an undetectable level of LPA_3 as judged by quantitative real-time RT-PCR (Fig. 1*B*). In the Boyden chamber assay, MSF cells migrated in response to LPA and the response was PTX-sensitive (Fig. 1*A*). We therefore examined LPA-induced cell motility in MSF cells isolated from previously established LPA receptor knock-out mice (20, 23). The migratory response was completely abolished in MSF cells isolated from $lpa_1^{-/-}$ mice (Fig. 2*A*). MSF cells from $lpa_2^{-/-}$ mice migrated normally in response to LPA (Fig. 2*A*). The $lpa_1^{-/-}$ MSF cells migrated normally in response to platelet-derived growth factor, a potent inducer of migration for fibroblasts (Fig. 2*B*), indicating that the $lpa_1^{-/-}$ cells have defects in their response to LPA but not migration *per se*. We also found that ATX stimulated the migration of MSF cells (Fig. 3) in a PTX-sensitive manner (data not shown). The migratory response induced by ATX also disappeared in MSF cells from $lpa_1^{-/-}$ mice but not from wild-type or $lpa_2^{-/-}$ mice (Fig. 3). These data demonstrated that of the three LPA receptors expressed in the MSF cells, LPA_1 is at least essential for LPA-stimulated cell migration. They also show that the motility effects of ATX are mediated by LPA signaling.

We next examined whether LPA_1 is involved in LPA- or ATX-induced cell motility of carcinoma cells by using various carcinoma cell lines that differentially express LPA receptors. LPA stimulated cell migration of multiple carcinoma cell lines, including MDA-MB-231 (breast cancer), PC-3 (prostate cancer), A-2058 (melanoma), A549 (lung cancer), ACHN (renal cancer), SF295 (glioblastoma), and SF539 (glioblastoma) (Fig. 4). Interestingly, these cells were found to express LPA_1 endogenously as judged by quantitative real-time RT-PCR (Fig. 4). LPA did not support the migration of MCF7 (breast cancer), HT-29 (colorectal cancer), KM-12 (colorectal cancer), OVCAR-4 (ovarian cancer), OVCAR-8 (ovarian cancer), NCI-H522 (lung

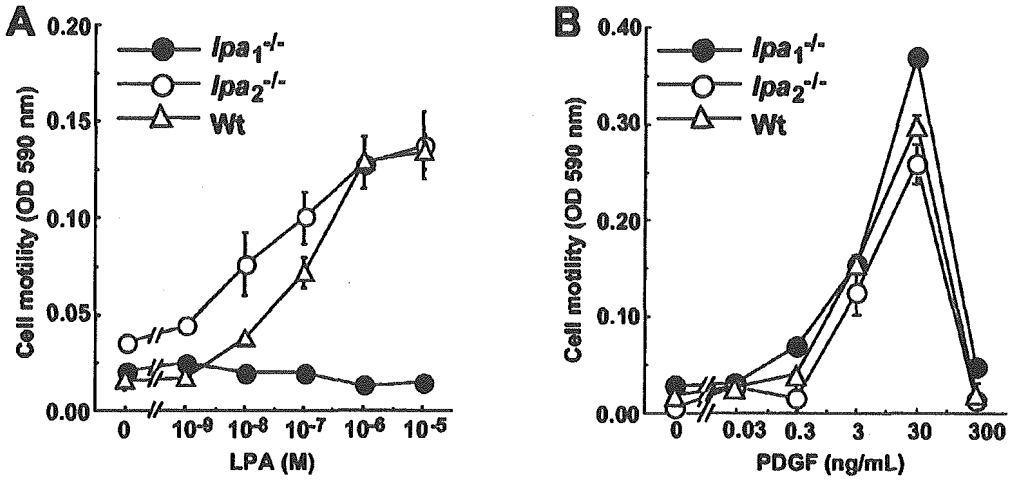

FIG. 2. **LPA$_1$ is essential for LPA-induced cell motility in mouse skin fibroblasts.** LPA-induced (*A*) and platelet-derived growth factor-induced (*B*) migration of MSF cells isolated from *lpa$_1$*$^{-/-}$ (*filled circles*), *lpa$_2$*$^{-/-}$ (*open circles*), and wild-type (*open triangles*) mice. Results shown are representative of at least three independent experiments. *Error bars* indicate the S.D. of the mean.

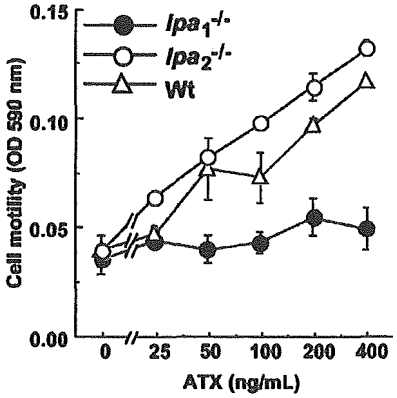

FIG. 3. **LPA$_1$ is essential for ATX-induced cell motility in mouse skin fibroblasts.** ATX-induced migration of MSF cells isolated from *lpa$_1$*$^{-/-}$ (*filled circles*), *lpa$_2$*$^{-/-}$ (*open circles*), and wild-type (*open triangles*) mice. Results shown are representative of at least three independent experiments. *Error bars* indicate the S.D. of the mean.

cancer), LNCaP (prostate cancer), and HeLa (cervical cancer) cells, and these cells did not appreciably express LPA$_1$ (Fig. 4). There was no obvious correlation between LPA-induced cell motility and expression of the three other LPA receptors, LPA$_2$, LPA$_3$, or LPA$_4$ (Fig. 4). ATX also induced migratory effects in LPA$_1$-expressing cells (Fig. 5) but not in cells that did not express LPA$_1$ (data not shown). Recently, an LPA$_1$-selective antagonist, Ki16425, (K_i values were 0.25 μM for LPA$_1$, 5.60 μM for LPA$_2$, and 0.36 μM for LPA$_3$) were developed (24). It has not been tested whether Ki16425 affects the activation of LPA$_4$. We then monitored intracellular calcium mobilization in HeLa cells transiently transfected with human and mouse LPA$_4$ cDNA and found that it was not inhibited by 1 μM Ki16425 (data not shown). Ki16425 inhibited the migratory response of LPA$_1$-expressing cells to both LPA and ATX (Figs. 4 and 5). Because Ki16425 is also a weak antagonist for LPA$_3$, it is possible that LPA$_3$ could be involved in the LPA- or ATX-stimulated cell motility of LPA$_3$-expressing cells. However, carcinoma cell lines expressing LPA$_3$ but not LPA$_1$ (OVCAR-8 and LNCaP) did not migrate in response to LPA (Fig. 4). In addition, OMPT, an LPA$_3$-selective agonist we recently developed (25), induced a smaller migratory response in A-2058 cells that express both LPA$_1$ and LPA$_3$, although LPA stimulated migration effectively (Fig. 6*A*). OMPT did activate intracellular calcium mobilization more effectively than LPA (Fig. 6*B*), indicating that OMPT activates LPA$_3$ in A-2058 cells. These results argue against the possibility that LPA$_3$ mediates LPA- or ATX-induced cell motility-stimulating activity. Thus, it can be concluded that LPA and ATX stimulate cell motility through LPA$_1$ but not through other LPA receptors, at least for the range of neoplastic cells examined here.

It is generally accepted that locomotion in cellular migration involves reorganization of the actin cytoskeleton as is observed in lamellipodia and stress fiber formation (26, 27). LPA signaling stimulates cytoskeletal reorganization in various cell types through activation of Rho GTPases. However, the molecular mechanisms underlined, particularly at receptor level, remained to be solved. We recently showed that LPA-induced stress fiber formation in mouse embryonic meningeal fibroblast cells (MEMFs) requires either LPA$_1$ or LPA$_2$ activation, based on the observation that it was severely affected in MEMFs from *lpa$_1$*$^{-/-}$*lpa$_2$*$^{-/-}$ mice but not in MEMFs from wild-type, *lpa$_1$*$^{-/-}$, and *lpa$_2$*$^{-/-}$ mice (20). In the present study, we tried to confirm the same effect in MSF cells derived from each LPA receptor knock-out mouse. However, we could not evaluate this in the MSF cells because abundant stress fibers were formed even in the absence of LPA. By contrast, we found that LPA-induced lamellipodia formation in MSF cells requires only LPA$_1$ expression. In wild-type and *lpa$_2$*$^{-/-}$ cells, LPA increased the number of cells with ruffling membranes (lamellipodia formation). In contrast, LPA did not affect the lamellipodia formation in *lpa$_1$*$^{-/-}$ and *lpa$_1$*$^{-/-}$*lpa$_2$*$^{-/-}$ MSF cells (Fig. 7, *A* and *B*).

The molecular control of actin filament assembly is dependent on the Rho family of small GTPases, particularly RhoA, Rac1, and Cdc42 (28). Rac1 regulates lamellipodia, whereas RhoA regulates the formation of contractile actin-myosin filaments to form stress fibers (28). LPA-stimulated migration of MSF cells was efficiently blocked by pretreatment of the cells with Y-27632 (data not shown), an inhibitor of Rho kinase that inactivates the RhoA pathway. We therefore measured the LPA-induced activation of the two small GTPases, Rac1 and RhoA, in MSF cells. Rac1 and RhoA were measured with GST-PAK and GST-Rhotekin pull-down assays, respectively. When MSF cells from wild-type and *lpa$_2$*$^{-/-}$ mice were stimulated with 1 μM LPA, a GTP-bound form of Rac1 was dramatically increased (Fig. 8). By contrast, Rac1 activation was almost completely abolished in both *lpa$_1$*$^{-/-}$ and *lpa$_1$*$^{-/-}$ *lpa$_2$*$^{-/-}$ MSF cells (Fig. 8). Although RhoA activation in response to LPA was obvious in wild-type and *lpa$_2$*$^{-/-}$ MSF cells, it appeared to be

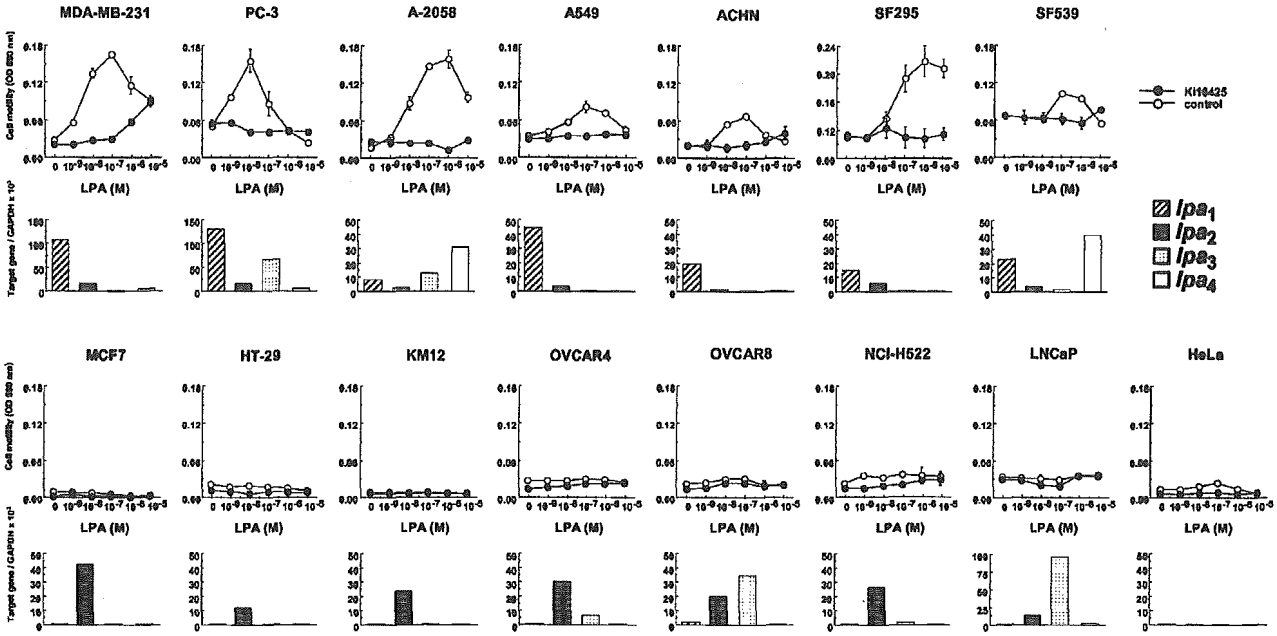

FIG. 4. **LPA$_1$ is involved in LPA-induced cell motility in multiple carcinoma cell lines.** In each cell line, the *upper panel* shows migratory response to LPA either in the absence (*open circles*) or presence (filled circles) of an LPA$_1$-selective antagonist, Ki16425 (1 μM), evaluated by the Boyden chamber assay. The *lower panel* shows expression of each LPA receptor mRNA (*lpa*$_1$, *lpa*$_2$, *lpa*$_3$, and *lpa*$_4$) measured using quantitative real-time RT-PCR. The LPA-induced migratory responses appear to be parallel with the expression of LPA$_1$.

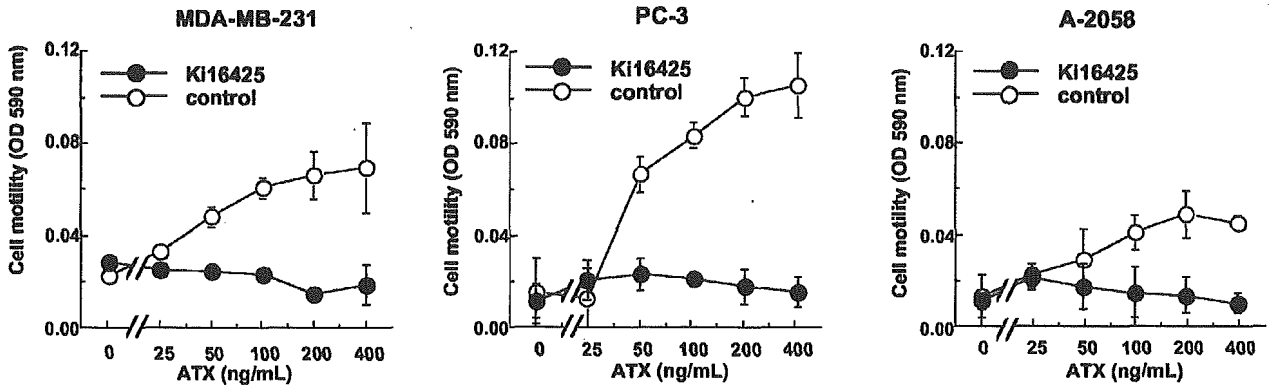

FIG. 5. **Ki16425 inhibits ATX-induced cell motility of carcinoma cell-expressing LPA$_1$.** ATX stimulates cell motility of three LPA$_1$-expressing carcinoma cell lines (MDA-MB-231, PC-3, and A-2058), and the motility is suppressed by an LPA$_1$-selective antagonist, Ki16425.

reduced in *lpa*$_1^{-/-}$ MSF cells and markedly reduced in *lpa*$_1^{-/-}$-*lpa*$_2^{-/-}$ MSF cells (Fig. 8). These results indicate that LPA$_1$ has a major role in both Rac1 and RhoA activation induced by LPA stimulation (Fig. 9). The Rac1 activation is predominantly dependent on LPA$_1$, whereas RhoA activation is less dependent on LPA$_1$. LPA$_2$ does contribute to the activation of RhoA in the absence of LPA$_1$ expression. In addition, RhoA can be activated to some extent (Fig. 8) in the absence of LPA$_1$ and LPA$_2$, indicating the presence of other LPA receptors and/or indirect mechanisms of RhoA activation (Fig. 9).

DISCUSSION

LPA is a multifunctional signaling molecule with diverse activities, including stimulation of cell motility. Recent identification of lysophospholipase D, an LPA-producing enzyme, as ATX, a cell-motility stimulating factor of cancer cells (10, 11), indicated that the activity is one of the intrinsic functions of LPA. In this study we showed that among the four LPA receptors identified so far, LPA$_1$ has a crucial role in LPA-induced cell migration of fibroblast cells (Fig. 2) and multiple cancer cells (Fig. 4), based on the observation that inactivation of LPA$_1$ either by gene-targeting technique or by a receptor-selective antagonist resulted in loss of migratory response. In addition, we observed that the migratory response induced by ATX again disappeared in these cells (Figs. 3 and 5). These results clearly show that ATX exerts its function through LPA production and the following LPA$_1$ activation. Both LPA$_1$ and ATX are highly expressed in brain (14, 29). Recently it was reported that oligodendrocytes express LPA$_1$ and ATX during myelination (30, 31). We also found that LPA$_1$ and ATX are highly enriched within certain regions of developing mouse brain, such as olfactory bulb.[2] The colocalization of the two genes suggests that they also function co-operatively in physiological condition.

The migratory responses were found to be PTX-sensitive (Fig. 1*A*). By contrast, in a previous report LPA was found to stimulate cell motility of other cell types, such as lymphoma

[2] M. Fukaya, M. Watanabe, J. Aoki, and H. Arai, unpublished result.

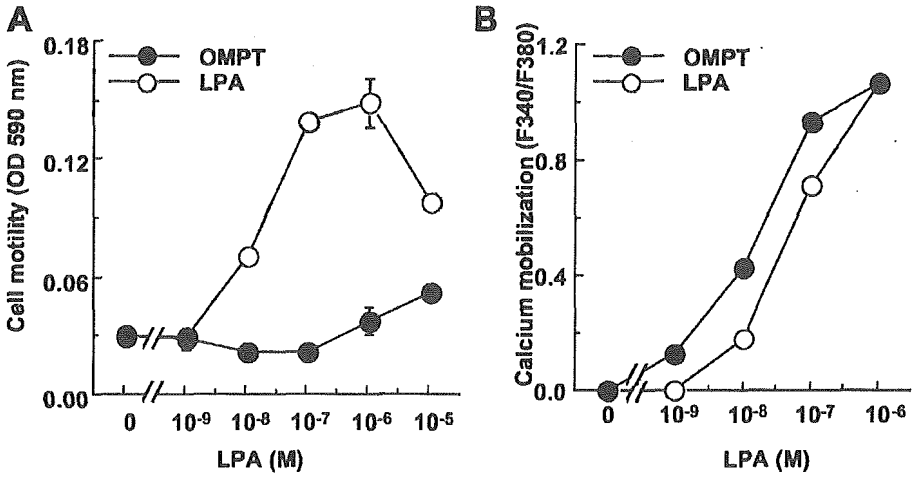

FIG. 6. **LPA$_3$ is not involved in LPA-induced cell motility.** *A*, OMPT did not stimulate cell motility of LPA$_3$-expressing cell, A-2058. *B*, OMPT induced an intracellular calcium mobilization of the cells more efficiently than LPA.

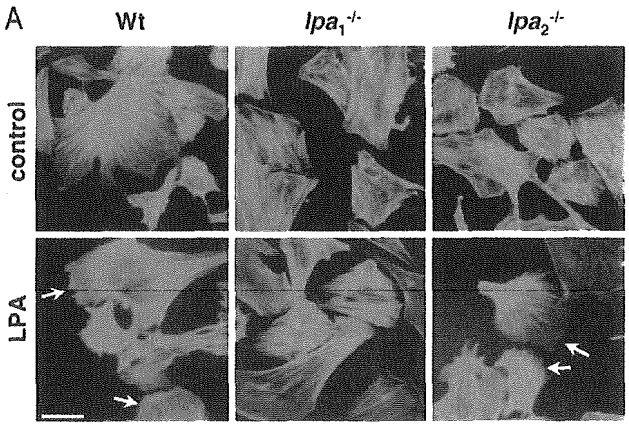

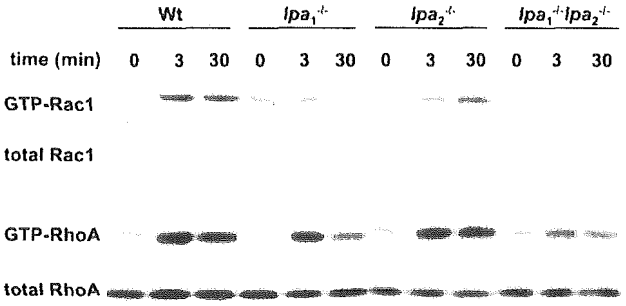

FIG. 8. **LPA-induced activation of Rac1 and RhoA in MSF cells.** MSF cells were serum-starved for 24 h and stimulated with 1 μM LPA. Activated RhoA and Rac1 were isolated using GST-PAK (*Rac1, upper panel*) or GST-Rhotekin (*RhoA, lower panel*) coupled to glutathione-Sepharose beads. Rac1 and RhoA bound to the beads were detected by Western blotting using specific antibodies.

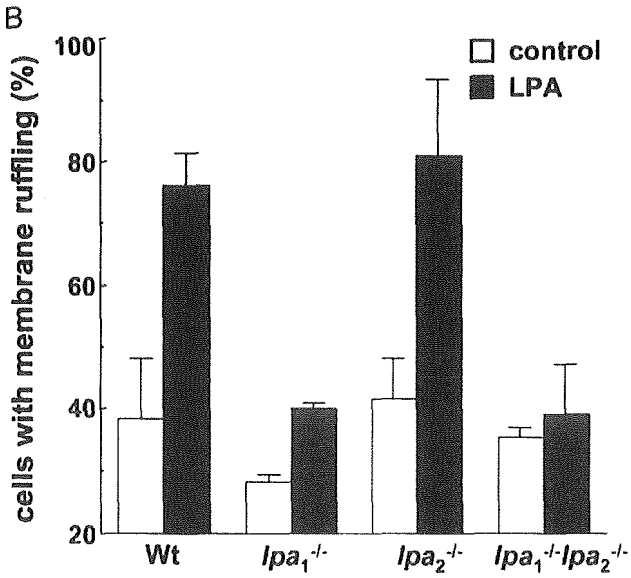

FIG. 7. **LPA induces lamellipodia formation through LPA$_1$.** *A*, fluorescence microscopy of BODIPY FL phallacidin-stained MSF cells from wild-type, *lpa*$_1$$^{-/-}$, and *lpa*$_2$$^{-/-}$ mice before (*upper panels*) or after (*lower panels*) LPA stimulation (1 μM, 3 h). The lamellipodia formation (*arrows*) was observed in wild-type and *lpa*$_2$$^{-/-}$ MSF cells but rarely observed in *lpa*$_1$$^{-/-}$ MSF cells. *Bar*, 20 μm. *B*, percentage of wild-type, *lpa*$_1$$^{-/-}$, *lpa*$_2$$^{-/-}$, and *lpa*$_1$$^{-/-}$ *lpa*$_2$$^{-/-}$ MSF cells with lamellipodia after stimulation with 1 μM LPA.

cells, in a PTX-insensitive manner (6). Because lymphocytes express LPA$_2$ predominantly with no detectable expression of LPA$_1$ (data not shown), it is possible that LPA$_2$ is involved in LPA-induced migratory response of non-carcinoma neoplasms, such as lymphoma cells. Splenocytes and thymocytes isolated from wild-type, *lpa*$_1$$^{-/-}$, *lpa*$_2$$^{-/-}$, and *lpa*$_1$$^{-/-}$ *lpa*$_2$$^{-/-}$ mice did not show a migratory response to LPA in our system (data not shown). In addition, in the absence of selective agonists or antagonists for LPA$_2$, we could not test the migratory effect of LPA$_2$ on lymphoma cell migration. Further study is necessary to show the role of LPA$_2$ in migratory response of lymphoma cells.

We previously showed that LPA$_1$ and LPA$_2$ had redundant functions in mediating multiple endogenous LPA responses, including phospholipase C activation, Ca^{2+} mobilization, cell proliferation, and stress fiber formation in mouse embryonic fibroblasts (20). In this study, we demonstrated that LPA-induced lamellipodia formation was severely affected in *lpa*$_1$$^{-/-}$ MSF cells (Fig. 7, *A* and *B*). In addition, we showed that LPA activates Rac1 in an LPA$_1$-dependent manner, whereas it activates RhoA either in LPA$_1$-, LPA$_2$-dependent or LPA$_1$-, LPA$_2$-independent pathway (Fig. 8). Thus, LPA$_1$ is able to activate both Rac1 and RhoA regardless of LPA$_2$ expression (Fig. 9). Because the activation of both RhoA and Rac1 is essential for LPA-stimulated cell migration (12), the lack of Rac1 activation in *lpa*$_1$$^{-/-}$ MSF cells explains why the cells could not migrate in response to LPA. Many reports have

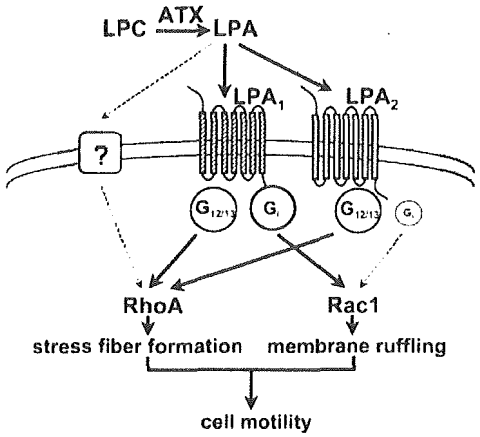

FIG. 9. **Model for LPA- or ATX-induced cell motility.** ATX activates Rac1 and RhoA through G_i and $G_{12/13}$, respectively, by producing LPA. The activation of Rac1 and RhoA results in membrane ruffling and stress fiber formation, which finally lead to activation of cell motility. The Rac1 activation is predominantly dependent on LPA_1, whereas RhoA activation is induced by either LPA_1 or LPA_2 activation. LPA_1- and LPA_2-independent pathways also contribute partially to RhoA activation.

shown that $G_{i/o}$ and $G_{12/13}$ regulate the activation of Rac1 and RhoA, respectively (12, 32). Thus, our results again suggest that LPA_1 couples with both $G_{i/o}$ and $G_{12/13}$, whereas LPA_2 mainly couples with $G_{12/13}$ as we indicated previously using cells transfected with each LPA receptor (Fig. 9) (20, 33). van Leeuwen *et al.* (12) recently showed that LPA_1, when overexpressed in B103 neuroblastoma cells, mediates LPA-induced cell migration through concomitant activation of Rac1. However, the role of other LPA receptors in cell motility remained to be solved, which we did in this study (Figs. 2 and 8). We showed that multiple carcinoma cells utilize the same mechanism for their LPA-induced cell motility (Fig. 4). It is well accepted that cell motility is closely linked to the metastatic and invasive potential of cancer cells. In addition, the activating pathways of both Rac1 and RhoA were also implicated in tumor invasion and metastasis (34, 35). Furthermore, there is accumulating evidence that elevated expression of ATX is observed in various cancer tissues (36, 37) and that the expression is closely linked to the invasive and metastatic potency of cancer cells (38). We therefore propose that both ATX and LPA_1 are the potential targets for cancer therapy.

Acknowledgments—We thank Dr. M. Negishi (Kyoto University) for advice on GST-pull-down assay and for the gift of GST-PAK and GST-RBD constructs and Drs. S. Ishii and T. Shimizu (University of Tokyo) for the generous gift of LPA_1 cDNA.

REFERENCES

1. Singer, S. J., and Kupfer, A. (1986) *Annu. Rev. Cell Biol.* **2,** 337–365
2. Friedl, P., and Wolf, K. (2003) *Nat. Rev. Cancer* **3,** 362–374
3. Moolenaar, W. H. (1999) *Exp. Cell Res.* **253,** 230–238
4. Contos, J. J., Ishii, I., and Chun, J. (2000) *Mol. Pharmacol.* **58,** 1188–1196
5. Manning, T. J., Parker, J. C., and Sontheimer, H. (2000) *Cell Motil. Cytoskeleton* **45,** 185–199
6. Stam, J. C., Michiels, F., van der Kammen, R. A., Moolenaar, W. H., and Collard, J. G. (1998) *EMBO J.* **17,** 4066–4074
7. Shida, D., Kitayama, J., Yamaguchi, H., Okaji, Y., Tsuno, N. H., Watanabe, T., Takuwa, Y., and Nagawa, H. (2003) *Cancer Res.* **63,** 1706–1711
8. Mills, G. B., and Moolenaar, W. H. (2003) *Nat. Rev. Cancer* **3,** 582–591
9. Stracke, M. L., Clair, T., and Liotta, L. A. (1997) *Adv. Enzyme Regul.* **37,** 135–144
10. Umezu, G. M., Kishi, Y., Taira, A., Hama, K., Dohmae, N., Takio, K., Yamori, T., Mills, G. B., Inoue, K., Aoki, J., and Arai, H. (2002) *J. Cell Biol.* **158,** 227–233
11. Tokumura, A., Majima, E., Kariya, Y., Tominaga, K., Kogure, K., Yasuda, K., and Fukuzawa, K. (2002) *J. Biol. Chem.* **277,** 39436–39442
12. van Leeuwen, F. N., Olivo, C., Grivell, S., Giepmans, B. N., Collard, J. G., and Moolenaar, W. H. (2003) *J. Biol. Chem.* **278,** 400–406
13. Stracke, M. L., Krutzsch, H. C., Unsworth, E. J., Arestad, A., Cioce, V., Schiffmann, E., and Liotta, L. A. (1992) *J. Biol. Chem.* **267,** 2524–2529
14. Hecht, J. H., Weiner, J. A., Post, S. R., and Chun, J. (1996) *J. Cell Biol.* **135,** 1071–1083
15. An, S., Bleu, T., Hallmark, O. G., and Goetzl, E. J. (1998) *J. Biol. Chem.* **273,** 7906–7910
16. Bandoh, K., Aoki, J., Hosono, H., Kobayashi, S., Kobayashi, T., Murakami, M. K., Tsujimoto, M., Arai, H., and Inoue, K. (1999) *J. Biol. Chem.* **274,** 27776–27785
17. Noguchi, K., Ishii, S., and Shimizu, T. (2003) *J. Biol. Chem.* **278,** 25600–25606
18. McIntyre, T. M., Pontsler, A. V., Silva, A. R., Hilaire, A., Xu, Y., Hinshaw, J. C., Zimmerman, G. A., Hama, K., Aoki, J., Arai, H., and Prestwich, G. D. (2003) *Proc. Natl. Acad. Sci. U. S. A.* **100,** 131–136
19. Hooks, S. B., Santos, W. L., Im, D. S., Heise, C. E., Macdonald, T. L., and Lynch, K. R. (2001) *J. Biol. Chem.* **276,** 4611–4621
20. Contos, J. J., Ishii, I., Fukushima, N., Kingsbury, M. A., Ye, X., Kawamura, S., Brown, J. H., and Chun, J. (2002) *Mol. Cell. Biol.* **22,** 6921–6929
21. Yamori, T., Matsunaga, A., Sato, S., Yamazaki, K., Komi, A., Ishizu, K., Mita, I., Edatsugi, H., Matsuba, Y., Takezawa, K., Nakanishi, O., Kohno, H., Nakajima, Y., Komatsu, H., Andoh, T., and Tsuruo, T. (1999) *Cancer Res.* **59,** 4042–4049
22. Yamaguchi, Y., Katoh, H., Yasui, H., Mori, K., and Negishi, M. (2001) *J. Biol. Chem.* **276,** 18977–18983
23. Contos, J. J., Fukushima, N., Weiner, J. A., Kaushal, D., and Chun, J. (2000) *Proc. Natl. Acad. Sci. U. S. A.* **97,** 13384–13389
24. Ohta, H., Sato, K., Murata, N., Damirin, A., Malchinkhuu, E., Kon, J., Kimura, T., Tobo, M., Yamazaki, Y., Watanabe, T., Yagi, M., Sato, M., Suzuki, R., Murooka, H., Sakai, T., Nishitoba, T., Im, D. S., Nochi, H., Tamoto, K., Tomura, H., and Okajima, F. (2003) *Mol. Pharmacol.* **64,** 994–1005
25. Hasegawa, Y., Erickson, J. R., Goddard, G. J., Yu, S., Liu, S., Cheng, K. W., Eder, A., Bandoh, K., Aoki, J., Jarosz, R., Schrier, A. D., Lynch, K. R., Mills, G. B., and Fang, X. (2003) *J. Biol. Chem.* **278,** 11962–11969
26. Lauffenburger, D. A., and Horwitz, A. F. (1996) *Cell* **84,** 359–369
27. Mitchison, T. J., and Cramer, L. P. (1996) *Cell* **84,** 371–379
28. Etienne, M. S., and Hall, A. (2002) *Nature* **420,** 629–635
29. Fuss, B., Baba, H., Phan, T., Tuohy, V. K., and Macklin, W. B. (1997) *J. Neurosci.* **23,** 9095–9103
30. Weiner, J. A., Hecht, J. H., and Chun, J. (1998) *J. Comp. Neurol.* **398,** 587–598
31. Fox, M. A., Colello, R. J., Macklin, W. J., and Fuss, B. (2003) *Mol. Cell. Neurosci.* **23,** 507–519
32. Kozasa, T., Jiang, X., Hart, M. J., Sternweis, P. M., Singer, W. D., Gilman, A. G., Bollag, G., and Sternweis, P. C. (1998) *Science* **280,** 2109–2111
33. Ishii, I., Contos, J. J., Fukushima, N., and Chun, J. (2001) *Mol. Pharmacol.* **58,** 895–902
34. Michiels, F., Habets, G. G., Stam, J. C., van der Kammen, R. A., and Collard, J. G. (1995) *Nature* **375,** 338–340
35. Itoh, K., Yoshioka, K., Akedo, H., Uehata, M., Ishizaki, T., and Narumiya, S. (1999) *Nat. Med.* **5,** 221–225
36. Yang, Y., Mou, L. J., Liu, N., and Tsao, M. S. (1999) *Am. J. Respir. Cell Mol. Biol.* **21,** 216–222
37. Zhang, G., Zhao, Z., Xu, S., Ni, L., and Wang, X. (1999) *Chin. Med. J.* **112,** 330–332
38. Yang, S. Y., Lee, J., Park, C. G., Kim, S., Hong, S., Chung, H. C., Min, S. K., Han, J. W., Lee, H. W., and Lee, H. Y. (2002) *Clin. Exp. Metastasis* **19,** 603–608

Oncogene (2004) 23, 289–297

www.nature.com/onc

Csk defines the ability of integrin-mediated cell adhesion and migration in human colon cancer cells: implication for a potential role in cancer metastasis

William Rengifo-Cam[1], Akio Konishi[1], Naoki Morishita[1], Hidetada Matsuoka[1], Takao Yamori[2], Shigeyuki Nada[1] and Masato Okada*[,1]

[1]*Department of Oncogene Research, Research Institute for Microbial Diseases, Osaka University, 3-1 Yamadaoka, Suita, 565-0871 Osaka, Japan;* [2]*Division of Molecular Pharmacology, Cancer Chemotherapy Center, Japanese Foundation for Cancer Research, Toshima-ku, Tokyo 170-8455, Japan*

Progression of human colon cancer is often associated with elevated expression and activity of the Src family tyrosine kinase (SFK). SFK is ordinarily in equilibrium between inactive and primed states by a balance of negative regulatory kinase Csk and its counteracting tyrosine phosphatase(s), both of which act on the regulatory C-terminal tyrosine of SFK. To evaluate the contribution of the regulatory system of SFK in cancer progression, we here modulated the equilibrium status of SFK by introducing wild-type or dominant-negative Csk in human epithelial colon cancer cells, HCT15 and HT29. Overexpression of wild-type Csk induced decreased SFK activation, increased cell–cell contacts mediated by E-cadherin, decreased the number of focal contacts and decreased cell adhesion/migration and *in vitro* invasiveness. Conversely, expression of a dominant-negative Csk resulted in elevated SFK activation, enhanced phosphorylation of FAK and paxilllin, enhanced cell scattering, an increased number of focal contacts, dramatic rearrangement of actin cytoskeleton and increased cell adhesion/migration and *in vitro* invasiveness. In these scattered cells, however, localization, expression and phosphorylation of either E-cadherin or β-catenin were not significantly affected, suggesting that the E-cadherin-mediated cell–cell contact is indirectly regulated by SFK. Furthermore, all these events occurred absolutely dependent on integrin-mediated cell adhesion. These findings demonstrate that Csk defines the ability of integrin-SFK-mediated cell adhesion signaling that influences the metastatic potential of cancer cells.
Oncogene (2004) **23**, 289–297. doi:10.1038/sj.onc.1207041

Keywords: Src; Csk; colon cancer; integrin

Introduction

The Src family tyrosine kinase (SFK) has been shown to play an important role in proliferation, differentiation, adhesion and migration of a variety of animal cells. These diverse functions are due to the pivotal role of SFK as membrane-attached molecular switches that link a variety of extracellular cues to crucial intracellular signaling pathways (Thomas and Brugge, 1997). The kinase activity of c-Src is known to be highly elevated in the majority of human colon cancers, and there is an increasing trend during further disease progression, with the highest values in metastasis disease (Talamonti *et al.*, 1993). In addition, some types of adenomas and ulcerative colitis, which possess a high risk of developing malignant disease, also course with increased c-Src activity (Cartwright *et al.*, 1994). This increased c-Src activity does not appear to result solely from an increase in the amount of the c-Src protein, suggesting that its specific activity is enhanced in some cases (Bolen *et al.*, 1987; Cartwright *et al.*, 1989). A subset of colon cancers has a nonsense mutation in the C-terminal regulatory domain of c-Src. This mutation has been demonstrated to be activating, tumorigenic and to promote metastasis (Irby *et al.*, 1999). However, since the frequency of this mutation appears to be very low, it seems unlikely to play a significant role in the progression of most colon cancers (Daigo *et al.*, 1999; Nilbert and Fernebro, 2000; Wang *et al.*, 2000; Laghi *et al.*, 2001). On the other hand, some cases of colon cancer have shown an upregulation of other members of SFK, such as Yes and Lck, suggesting that SFK upregulation in cancer cells might be a more common event (Veillette *et al.*, 1987; Boardman and Karnes, 1995).

The C-terminal Src kinase (Csk) is a cytoplasmic tyrosine kinase that serves as an essential and a common negative regulator of SFK through specific phosphorylation at the C-terminal regulatory site of SFK (Tyr-529 in human c-Src) (Okada and Nakagawa, 1989; Nada *et al.*, 1991). The phosphorylated C-terminal tyrosine binds intramolecularly to the SH2 domain of SFK, thereby generating an inactive conformation (Okada *et al.*, 1991; Sabe *et al.*, 1992a). The importance of Csk as a negative regulator for SFK and the absence of functional redundancy have been demonstrated by the observation that Csk knockout mice, which are lethal at prenatal stage, exhibited constitutive activation of multiple SFK members (Imamoto and Soriano, 1993; Nada *et al.*, 1993). It is

*Correspondence: M Okada; E-mail: okadam@biken.osaka-u.ac.jp
Received 9 May 2003; revised 28 June 2003; accepted 24 July 2003